Available online at www.sciencedirect.com
ScienceDirect
International Journal of Mechanical Sciences 49 (2007) 669–689
International Journal of MECHANICAL SCIENCES
www.elsevier.com/locate/ijmecsci

Three-dimensional solutions of multilayered piezoelectric hollow cylinders by an asymptotic approach

Chih-Ping Wu[a,*], Yun-Siang Syu[a], Jyh-Yeuan Lo[b]

[a]*Department of Civil Engineering, National Cheng Kung University, Taiwan, ROC*
[b]*Department of Sports Business, Aletheia University, Taiwan, ROC*

Received 9 July 2006; received in revised form 4 November 2006; accepted 12 November 2006
Available online 28 December 2006

Abstract

Three-dimensional (3D) solutions for the static analysis of multilayered piezoelectric hollow cylinders are presented by means of an asymptotic approach. Either applied load or applied electric potential on the lateral surfaces is considered. The edge conditions of the cylinders are considered as simple supports. In the present formulation, the 22 basic equations in a cylindrical coordinates system are firstly reduced to eight differential equations in terms of eight primary variables of elastic and electric fields. After the mathematical derivation of nondimensionalization, asymptotic expansion and successive integration, we obtained recurrent sets of governing equations for various order problems. In view of the recurrent property, the present asymptotic solutions can be obtained in a hierarchic manner and asymptotically approach the 3D piezoelectricity solutions. Several benchmark problems of single-layer and multilayered piezoelectric hollow cylinders are studied using the present asymptotic formulation.

Keywords: Piezoelectric material; Cylinders; 3D solutions; Piezoelectricity; Asymptotic expansion

1. Introduction

In recent years, multilayered piezoelectric structures (i.e., laminated composite structures bonded with piezoelectric actuators and sensors on the outer surfaces of the structures) were widely used as intelligent or smart structures in the engineering applications in view of their capabilities of sensing, processing/control and actuating. It was further reported that these hybrid piezoelectric structures would improve the performance and reliability of laminated composite structures. Hence, determination of exact solutions for the static and dynamic behavior of piezoelectric laminates naturally attracts the researchers' attention and becomes an attractive research subject.

Several exact and accurate solutions of single-layer and multilayered hybrid piezoelectric structures have been presented in the literature. Heyliger [1,2] presented exact solutions for the static analysis of hybrid plates containing both piezoelectric and elastic layers under applied loads and applied potentials on the outer surfaces. In Heyliger's analysis, the primary field variables have been expanded as Fourier series in the in-surface directions. By using these doubly Fourier series functions, Heyliger reduced the three-dimensional (3D) basic equations as a set of ordinary differential equations. Power series expansion method has been used to evaluate the coupling effects of elastic and electric fields on the structural behavior of hybrid piezoelectric plates. The coupled thermoelectroelastic response of multilayered hybrid composite plates was presented by Xu et al. [3]. The effects of variation in the geometric parameters of the plates on the field variables were studied.

Dumir et al. [4] and Dube et al. [5] presented the exact piezoelastic and piezothermoelastic solutions, respectively, of infinitely long, simply-supported orthotropic circular cylindrical panels in cylindrical bending. In combination with the methods of separating variables and Fourier series expansion, 3D equations have been reduced to Euler–Cauchy type of ordinary differential equations. After solving the resulting equations by means of the Frobenius method and then imposing the appropriate lateral boundary

*Corresponding author. Tel.: +886 6 2757575; fax: +886 6 2370804.
E-mail address: cpwu@mail.ncku.edu.tw (C.-P. Wu).

0020-7403/$ - see front matter © 2006 Elsevier Ltd. All rights reserved.
doi:10.1016/j.ijmecsci.2006.11.002

conditions and interfacial continuity conditions, several benchmark solutions of the corresponding problems have been determined.

Chen et al. [6] presented exact solutions of piezoelectric cylindrical strips under cylindrical bending. The electric charge and potential of piezoelectric layers induced by applying mechanical loads and the deformations of piezoelectric layers induced by applying electric potentials, have been studied. Chen et al. [7] studied for the 3D analysis of piezoelectric cylindrical panels with finite length. The variations of various elastic and electric field variables through the thickness of the panels for different values of the radius-to-thickness ratios have been mainly concerned. Heyliger [8] presented the 3D solutions of laminated piezoelectric hollow cylinders under the applied mechanical or electric loads in the form of one term doubly Fourier series.

Kapuria et al. [9,10] and Xu et al. [11] presented 3D piezoelastic solution of multilayered cylindrical shells under static electromechanical loads using the modified Frobenius method. The primary field variables have been constructed in the form of a product of an exponential function and a power series in the thickness coordinate. It has been concluded that the modified Frobenius method yields better convergence properties.

The assessment of classical shell theory (CST) and first-order shear deformation theory (FSDT) for hybrid piezoelectric cylindrical shells was made by Kapuria et al. [12]. Comprehensive reviews of theoretical analysis and numerical modeling for piezoelectric laminates were presented by Gopinathan et al. [13] and Chee et al. [14].

An alternative analytical approach to obtain 3D elasticity solutions of various laminates was proposed by Wu and his colleagues [15–17]. By means of the perturbation method, the 3D asymptotic formulations for the static, dynamic and nonlinear analyses of laminated composite shells were developed. The 3D asymptotic solutions corresponding to various benchmark problems of laminated composite shells have been presented and illustrated to be in excellent agreement with the accurate solutions available in the literature.

The purpose of the present paper is to extend the asymptotic theory to multilayered piezoelectric hollow cylinders. In view of the coupling effect of elastic and electric fields, the present asymptotic formulation is inherently more complicated than that in early papers. Nevertheless, we shall see that the derivation is complicated but straightforward and consistent. The 3D solutions for the benchmark problems of single-layer and multilayered piezoelectric hollow cylinders under electric potential excitation can be determined in a systematic and hierarchic way. The coupling effects of elastic and piezoelectric fields on the structural behavior of single-layer and multilayered piezoelectric cylinders are studied.

2. Basic equations of piezoelectricity

Consider a piezoelectric hollow cylinder as shown in Fig. 1. The cylindrical coordinates system with variables x, θ, r is used and located on the middle surface of the hollow cylinder. $2h$, L and R stand for the total thickness, the length and the curvature radii to the middle surface of the hollow cylinder, respectively.

The linear constitutive equations valid for the nature of symmetry class of piezoelectric material are given by

$$\begin{Bmatrix} \sigma_x \\ \sigma_\theta \\ \sigma_r \\ \tau_{\theta r} \\ \tau_{xr} \\ \tau_{x\theta} \end{Bmatrix} = \begin{bmatrix} c_{11} & c_{12} & c_{13} & 0 & 0 & c_{16} \\ c_{12} & c_{22} & c_{23} & 0 & 0 & c_{26} \\ c_{13} & c_{23} & c_{33} & 0 & 0 & c_{36} \\ 0 & 0 & 0 & c_{44} & c_{45} & 0 \\ 0 & 0 & 0 & c_{45} & c_{55} & 0 \\ c_{16} & c_{26} & c_{36} & 0 & 0 & c_{66} \end{bmatrix} \begin{Bmatrix} \varepsilon_x \\ \varepsilon_\theta \\ \varepsilon_r \\ \gamma_{\theta r} \\ \gamma_{xr} \\ \gamma_{x\theta} \end{Bmatrix}$$

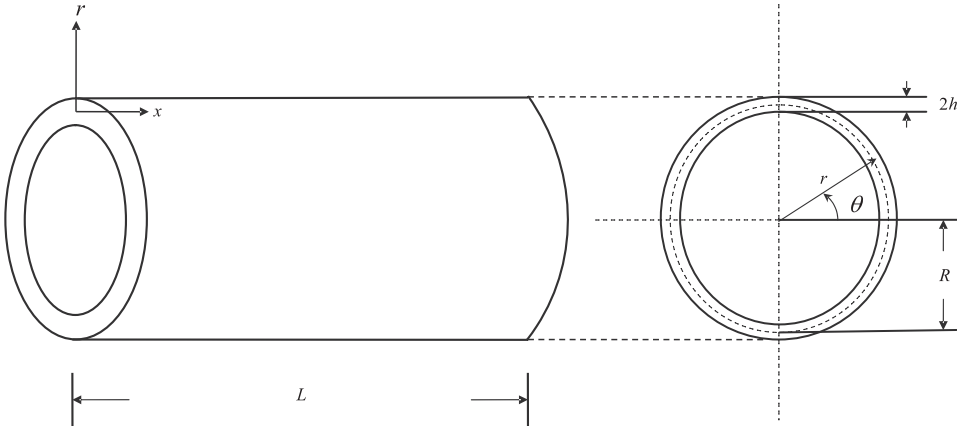

Fig. 1. The geometry and coordinates of a typical hollow cylinder.

$$-\begin{bmatrix} 0 & 0 & e_{31} \\ 0 & 0 & e_{32} \\ 0 & 0 & e_{33} \\ e_{14} & e_{24} & 0 \\ e_{15} & e_{25} & 0 \\ 0 & 0 & e_{36} \end{bmatrix} \begin{Bmatrix} E_x \\ E_\theta \\ E_r \end{Bmatrix}, \tag{1}$$

$$\begin{Bmatrix} D_x \\ D_\theta \\ D_r \end{Bmatrix} = \begin{bmatrix} 0 & 0 & 0 & e_{14} & e_{15} & 0 \\ 0 & 0 & 0 & e_{24} & e_{25} & 0 \\ e_{31} & e_{32} & e_{33} & 0 & 0 & e_{36} \end{bmatrix} \begin{Bmatrix} \varepsilon_x \\ \varepsilon_\theta \\ \varepsilon_r \\ \gamma_{\theta r} \\ \gamma_{xr} \\ \gamma_{x\theta} \end{Bmatrix} + \begin{bmatrix} \eta_{11} & \eta_{12} & 0 \\ \eta_{12} & \eta_{22} & 0 \\ 0 & 0 & \eta_{33} \end{bmatrix} \begin{Bmatrix} E_x \\ E_\theta \\ E_r \end{Bmatrix}, \tag{2}$$

where $\sigma_x, \sigma_\theta, \sigma_r, \tau_{xr}, \tau_{\theta r}, \tau_{x\theta}$ and $\varepsilon_x, \varepsilon_\theta, \varepsilon_r, \gamma_{xr}, \gamma_{\theta r}, \gamma_{x\theta}$ denote the stress and strain components, respectively. D_x, D_θ, D_r and E_x, E_θ, E_r denote the components of electric displacement and electric fields, respectively. c_{ij}, e_{ij} and η_{ij} are the elastic coefficients, piezoelectric coefficients and dielectric coefficients, respectively, relative to the geometrical axes of the hollow cylinder. The material is regarded to be heterogeneous through the thickness (i.e., $c_{ij}(\zeta)$, $e_{ij}(\zeta)$ and $\eta_{ij}(\zeta)$) and to be the layerwise step functions through the thickness direction.

The kinematic equations in terms of the cylindrical coordinates x, θ and r are

$$\varepsilon_x = \frac{\partial u_x}{\partial x}, \quad \varepsilon_\theta = \frac{1}{r}\left(\frac{\partial u_\theta}{\partial \theta} + u_r\right), \quad \varepsilon_r = \frac{\partial u_r}{\partial r},$$

$$\gamma_{xr} = \frac{\partial u_x}{\partial r} + \frac{\partial u_r}{\partial x}, \quad \gamma_{\theta r} = \frac{\partial u_\theta}{\partial r} - \frac{u_\theta}{r} + \frac{1}{r}\frac{\partial u_r}{\partial \theta},$$

$$\gamma_{x\theta} = \frac{1}{r}\frac{\partial u_x}{\partial \theta} + \frac{\partial u_\theta}{\partial x}, \tag{3a–f}$$

in which u_x, u_θ and u_r are the displacement components.

The stress equilibrium equations without body forces in the cylindrical coordinates system are given by

$$r\frac{\partial \sigma_x}{\partial x} + \frac{\partial \tau_{x\theta}}{\partial \theta} + \tau_{xr} + r\frac{\partial \tau_{xr}}{\partial r} = 0, \tag{4}$$

$$\gamma\frac{\partial \tau_{x\theta}}{\partial x} + \frac{\partial \sigma_\theta}{\partial \theta} + r\frac{\partial \tau_{\theta r}}{\partial r} + 2\tau_{\theta r} = 0, \tag{5}$$

$$r\frac{\partial \tau_{xr}}{\partial x} + \frac{\partial \tau_{\theta r}}{\partial \theta} + r\frac{\partial \sigma_r}{\partial r} + \sigma_r - \sigma_\theta = 0. \tag{6}$$

The charge equation of the piezoelectric material without electric charge density in the cylindrical coordinates system is

$$\frac{\partial D_x}{\partial x} + \frac{1}{r}\frac{\partial D_\theta}{\partial \theta} + \frac{\partial D_r}{\partial r} + \frac{D_r}{r} = 0. \tag{7}$$

The relations between the electric field and electric potential in the cylindrical coordinates system are

$$E_x = -\frac{\partial \Phi}{\partial x}, \tag{8a}$$

$$E_\theta = -\frac{1}{r}\frac{\partial \Phi}{\partial \theta}, \tag{8b}$$

$$E_r = -\frac{\partial \Phi}{\partial r}, \tag{8c}$$

where Φ denotes the electric potential.

The boundary conditions of the problem are specified as follows:

On the lateral surface the transverse load $\overline{q}_r^{\pm}(x, \theta)$ and electric potential $\overline{\Phi}^{\pm}(x, \theta)$ are prescribed,

$$[\tau_{xr} \ \ \tau_{\theta r}] = [0 \ \ 0] \quad \text{on } r = R \pm h, \tag{9a}$$

$$\sigma_r = \overline{q}_r{}^{\pm}(x, \ \theta) \quad \text{on } r = R \pm h, \tag{9b}$$

$$\Phi = \overline{\Phi}^{\pm}(x, \ \theta) \quad \text{on } r = R \pm h. \tag{10}$$

The edge boundary conditions require one member of each pair of the following quantities be satisfied:

$$n_1\sigma_x + n_2\tau_{x\theta} = p_1 \quad \text{or} \quad u_x = \overline{u}_x, \tag{11a}$$

$$n_1\tau_{x\theta} + n_2\sigma_\theta = p_2 \quad \text{or} \quad u_\theta = \overline{u}_\theta, \tag{11b}$$

$$n_1\tau_{xr} + n_2\tau_{\theta r} = p_3 \quad \text{or} \quad u_r = \overline{u}_r, \tag{11c}$$

where p_1, p_2 and p_3 are the applied edge loads; $\overline{u}_x, \overline{u}_\theta$ and $\overline{u}_r$ are the prescribed edge displacements; n_1 and n_2 denote the outward unit normal at a point along the edge.

In addition, the edges are suitably grounded so that the electric potential Φ at the edges are zero and given by

$$\Phi = 0. \tag{12}$$

According to Eqs. (1)–(8), it is listed that there are 22 basic equations for the present electroelastic analysis of hybrid piezoelectric hollow cylinders. For a 3D analysis, we must determine the aforementioned 22 unknown variables satisfying the basic equations (Eqs. (1)–(8) in the shell domain, the boundary conditions at outer surfaces (Eqs. (9)–(10)) and the edges (Eqs. (11)–(12)). In the following derivation, we present an asymptotic formulation for the 3D analysis of single-layer and multilayered hybrid piezoelectric hollow cylinders.

3. Nondimensionalization

A set of dimensionless coordinates and variables are defined as

$$x_1 = x/R \in, \quad x_2 = \theta/ \in, \ x_3 = \zeta/h \quad \text{and } r = R + \zeta;$$

$$u_1 = u_x/R \in, \quad u_2 = u_\theta/R \in, \ u_3 = u_r/R;$$

$$\sigma_1 = \sigma_x/Q, \quad \sigma_2 = \sigma_\theta/Q, \ \tau_{12} = \tau_{x\theta}/Q;$$

$$\tau_{13} = \tau_{xr}/Q \in, \quad \tau_{23} = \tau_{\theta r}/Q \in, \quad \sigma_3 = \sigma_r/Q\in^2;$$

$$D_1 = D_x/e \in, \quad D_2 = D_\theta/e \in, \ D_3 = D_r/e;$$

$$\phi = \Phi e/hQ; \tag{13a–g}$$

where $\in^2 = h/R$; Q and e denote a reference elastic moduli and a reference piezoelectric moduli, respectively.

By eliminating the in-surface stresses $(\sigma_x, \sigma_\theta, \tau_{x\theta})$, electric displacements (D_x and D_θ), the components of strain $(\varepsilon_x, \varepsilon_\theta, \varepsilon_r, \gamma_{xr}, \gamma_{\theta r}, \gamma_{x\theta})$ and electric fields (E_x, E_θ, E_r) from Eqs. (1)–(8), and then introducing the set of dimensionless coordinates and variables (Eq. (13)) in the resulting equations, we can rewrite the basic equations in the form of:

$$u_{3,3} = -\in^2 \mathbf{L}_1\mathbf{u} - \in^2 \tilde{l}_{33}u_3 + \in^4 \tilde{l}_{34}\sigma_3 + \in^2 \tilde{l}_{35}D_3, \tag{14}$$

$$\mathbf{u},_3 = -\mathbf{D}u_3 + \in^2 \mathbf{L}_2\mathbf{u} + \in^2 \mathbf{S}\boldsymbol{\sigma}_s + \in^4 \mathbf{L}_3\boldsymbol{\sigma}_s + \in^2 \mathbf{L}_4\phi, \tag{15}$$

$$D_{3,3} = -\in^2 \mathbf{L}_{11}\mathbf{d} - \in^2 \tilde{l}_{71}D_3, \tag{16}$$

$$\boldsymbol{\sigma}_s,_3 = -\mathbf{L}_5\mathbf{u} - \mathbf{L}_6u_3 - \in^2 \mathbf{L}_7\boldsymbol{\sigma}_s - \in^2 \gamma_\theta \mathbf{L}_1^{\mathrm{T}}\sigma_3 - \mathbf{L}_8D_3, \tag{17}$$

$$\sigma_3,_3 = \mathbf{L}_9\mathbf{u} + \tilde{l}_{63}u_3 - \mathbf{D}^{\mathrm{T}}\boldsymbol{\sigma}_s - \in^2 \mathbf{L}_{10}\boldsymbol{\sigma}_s - \in^2 \tilde{l}_{64}\sigma_3 + \tilde{l}_{65}D_3, \tag{18}$$

$$\phi,_3 = -(1/\gamma_\theta)\mathbf{L}_8^{\mathrm{T}}\mathbf{u} - (1/\gamma_\theta)\tilde{l}_{65}u_3 + \in^2 \tilde{l}_{35}\sigma_3 + \tilde{l}_{81}D_3, \tag{19}$$

where

$$\mathbf{u} = \begin{Bmatrix} u_1 \\ u_2 \end{Bmatrix}, \quad \mathbf{D} = \begin{Bmatrix} \partial_1 \\ \partial_2 \end{Bmatrix}, \ \mathbf{S} = \begin{bmatrix} \tilde{l}_{14} & \tilde{l}_{15} \\ \tilde{l}_{15} & \tilde{l}_{25} \end{bmatrix},$$

$$\boldsymbol{\sigma}_s = \begin{Bmatrix} \tau_{13} \\ \tau_{23} \end{Bmatrix}, \quad \mathbf{d} = \begin{Bmatrix} D_1 \\ D_2 \end{Bmatrix},$$

$$\mathbf{L}_1 = [\tilde{l}_{31} \ \ \tilde{l}_{32}], \quad \mathbf{L}_2 = \begin{bmatrix} 0 & 0 \\ 0 & \tilde{l}_{22} \end{bmatrix},$$

$$\mathbf{L}_3 = \begin{bmatrix} 0 & 0 \\ \tilde{l}_{26} & \tilde{l}_{27} \end{bmatrix}, \quad \mathbf{L}_4 = \begin{bmatrix} \tilde{l}_{18} \\ \tilde{l}_{28} \end{bmatrix},$$

$$\mathbf{L}_5 = \begin{bmatrix} \tilde{l}_{41} & \tilde{l}_{42} \\ \tilde{l}_{51} & \tilde{l}_{52} \end{bmatrix}, \quad \mathbf{L}_6 = \begin{bmatrix} \tilde{l}_{43} \\ \tilde{l}_{53} \end{bmatrix}, \ \mathbf{L}_7 = \begin{bmatrix} \tilde{l}_{44} & 0 \\ 0 & \tilde{l}_{55} \end{bmatrix},$$

$$\mathbf{L}_8 = \begin{bmatrix} \tilde{l}_{46} \\ \tilde{l}_{56} \end{bmatrix},$$

$$\mathbf{L}_9 = [\tilde{l}_{61} \ \ \tilde{l}_{62}], \quad \mathbf{L}_{10} = [x_3\partial_1 \ \ 0], \ \mathbf{L}_{11} = \begin{bmatrix} \partial_1 & \dfrac{1}{\gamma_\theta}\partial_2 \end{bmatrix},$$

$\gamma_\theta = 1 + \in^2 x_3$, and $\tilde{l}_{ij}$ are given in Appendix A.

It is noted that in the resulting equations (Eqs. (14)–(19)) all the differential operators on the left-hand sides are with respect to x_3 only, whereas on the right-hand sides are with respect to x_1 and x_2.

The in-surface stresses and electric displacements can be expressed in terms of the primary variables as follows:

$$\boldsymbol{\sigma}_p = \mathbf{B}_1\mathbf{u} + \mathbf{B}_2u_3 + \in^2 \mathbf{B}_3\sigma_3 + \mathbf{B}_4D_3, \tag{20}$$

$$\mathbf{d} = \mathbf{B}_5\boldsymbol{\sigma}_s + \mathbf{B}_6\phi, \tag{21}$$

where

$$\boldsymbol{\sigma}_p = \begin{Bmatrix} \sigma_1 \\ \sigma_2 \\ \tau_{12} \end{Bmatrix}, \quad \mathbf{B}_1 = \begin{bmatrix} \tilde{b}_{11} & \tilde{b}_{12} \\ \tilde{b}_{21} & \tilde{b}_{22} \\ \tilde{b}_{31} & \tilde{b}_{32} \end{bmatrix}, \ \mathbf{B}_2 = \begin{bmatrix} \tilde{b}_{13} \\ \tilde{b}_{23} \\ \tilde{b}_{33} \end{bmatrix},$$

$$\mathbf{B}_3 = \begin{bmatrix} \tilde{b}_{14} \\ \tilde{b}_{24} \\ \tilde{b}_{34} \end{bmatrix}, \quad \mathbf{B}_4 = \begin{bmatrix} \tilde{b}_{15} \\ \tilde{b}_{25} \\ \tilde{b}_{35} \end{bmatrix}, \ \mathbf{B}_5 = \begin{bmatrix} \tilde{b}_{41} & \tilde{b}_{42} \\ \tilde{b}_{51} & \tilde{b}_{52} \end{bmatrix},$$

$$\mathbf{B}_6 = \begin{bmatrix} \tilde{b}_{43} \\ \tilde{b}_{53} \end{bmatrix},$$

and $\tilde{b}_{ij}$ are given in Appendix A.

The dimensionless form of boundary conditions of the problem are specified as follows:

On the lateral surface the transverse load and electric potential are prescribed,

$$[\tau_{13} \ \ \tau_{23}] = [0 \ \ 0] \quad \text{on } x_3 = \pm 1, \tag{22a}$$

$$\sigma_3 = \overline{q}_3^{\pm}(x_1, \ x_2) \quad \text{on } x_3 = \pm 1, \tag{22b}$$

$$\phi = \overline{\phi}^{\pm}(x_1, \ x_2) \quad \text{on } x_3 = \pm 1. \tag{23}$$

At the edges one member of each pair of the following quantities is satisfied:

$$n_1\sigma_1 + n_2\tau_{12} = p_{n1} \quad \text{or} \quad u_1 = \overline{u}_1, \tag{24a}$$

$$n_1\tau_{12} + n_2\sigma_2 = p_{n2} \quad \text{or} \quad u_2 = \overline{u}_2, \tag{24b}$$

$$n_1\tau_{13} + n_2\tau_{23} = p_{n3} \quad \text{or} \quad u_3 = \overline{u}_3. \tag{24c}$$

In addition,

$$\phi = 0, \tag{25}$$

where $\overline{q}_3{}^{\pm} = \overline{q}_r{}^{\pm}/Q\in^2$; $\overline{\phi}^{\pm} = \overline{\Phi}^{\pm}e/hQ$; $(p_{n1}, p_{n2}, p_{n3}) = (p_1/Q, p_2/Q, p_3/Q \in)$; $(\overline{u}_1, \overline{u}_2, \overline{u}_3) = (\overline{u}_x/R \in, \overline{u}_\theta/R \in, \overline{u}_r/R)$.

4. Asymptotic expansions

Since Eqs. (14)–(19) contain terms involving only even powers of $\in$, we therefore asymptotically expand the primary variables in the powers $\in^2$ as given by

$$f(x_1, x_2, x_3, \in) = f^{(0)}(x_1, x_2, x_3) + \in^2 f^{(1)}(x_1, x_2, x_3) + \in^4 f^{(2)}(x_1, x_2, x_3) + \cdots . \tag{26}$$

Substituting Eq. (26) into Eqs. (14)–(19) and collecting coefficients of equal powers of $\in$, we obtain the following sets of recurrence equations.

Order $\in^0$:

$$u_3^{(0)},_3 = 0, \tag{27}$$

$$\mathbf{u}^{(0)},_3 = -\mathbf{D}u_3^{(0)}, \tag{28}$$

$$D_3^{(0)},_3 = 0, \tag{29}$$

$$\boldsymbol{\sigma}_s^{(0)},_3 = -\mathbf{L}_5\mathbf{u}^{(0)} - \mathbf{L}_6u_3^{(0)} - \mathbf{L}_8D_3^{(0)}, \tag{30}$$

$$\sigma_3^{(0)},_3 = \mathbf{L}_9\mathbf{u}^{(0)} + \tilde{l}_{63}u_3^{(0)} - \mathbf{D}^{\mathrm{T}}\boldsymbol{\sigma}_s^{(0)} + \tilde{l}_{65}D_3^{(0)}, \tag{31}$$

$$\phi^{(0)},_3 = -(1/\gamma_\theta)\mathbf{L}_8^{\mathrm{T}}\mathbf{u}^{(0)} - (1/\gamma_\theta)\tilde{l}_{65}u_3^{(0)} + \tilde{l}_{81}D_3^{(0)}, \tag{32}$$

$$\boldsymbol{\sigma}_p^{(0)} = \mathbf{B}_1\mathbf{u}^{(0)} + \mathbf{B}_2u_3^{(0)} + \mathbf{B}_4D_3^{(0)}, \tag{33}$$

$$\mathbf{d}^{(0)} = \mathbf{B}_5\boldsymbol{\sigma}_s^{(0)} + \mathbf{B}_6\phi^{(0)}, \tag{34}$$

Order $\in^{2k}$ ($k = 1, 2, 3$, etc.):

$$u_3^{(k)},_3 = -\mathbf{L}_1\mathbf{u}^{(k-1)} - \tilde{l}_{33}u_3^{(k-1)} + \tilde{l}_{34}\sigma_3^{(k-2)} + \tilde{l}_{35}D_3^{(k-1)}, \tag{35}$$

$$\mathbf{u}^{(k)},_3 = -\mathbf{D}u_3^{(k)} + \mathbf{L}_2\mathbf{u}^{(k-1)} + \mathbf{S}\boldsymbol{\sigma}_s^{(k-1)} + \mathbf{L}_3\boldsymbol{\sigma}_s^{(k-2)} + \mathbf{L}_4\phi^{(k-1)}, \tag{36}$$

$$\boldsymbol{\sigma}_s^{(k)},_3 = -\mathbf{L}_5\mathbf{u}^{(k)} - \mathbf{L}_6u_3^{(k)} - \mathbf{L}_7\boldsymbol{\sigma}_s^{(k-1)} - \gamma_0\mathbf{L}_1^{\mathrm{T}}\sigma_3^{(k-1)} - \mathbf{L}_8D_3^{(k)}, \tag{37}$$

$$\sigma_3^{(k)},_3 = \mathbf{L}_9\mathbf{u}^{(k)} + \tilde{l}_{63}u_3^{(k)} - \mathbf{D}^{\mathrm{T}}\boldsymbol{\sigma}_s^{(k)} - \mathbf{L}_{10}\boldsymbol{\sigma}_s^{(k-1)} - \tilde{l}_{64}\sigma_3^{(k-1)} + \tilde{l}_{65}D_3^{(k)}, \tag{38}$$

$$D_3^{(k)},_3 = -\mathbf{L}_{11}\mathbf{d}^{(k-1)} - \tilde{l}_{71}D_3^{(k-1)}, \tag{39}$$

$$\phi^{(k)},_3 = -(1/\gamma_\theta)\mathbf{L}_8^{\mathrm{T}}\mathbf{u}^{(k)} - (1/\gamma_\theta)\tilde{l}_{65}u_3^{(k)} + \tilde{l}_{35}\sigma_3^{(k-1)} + \tilde{l}_{81}D_3^{(k)}, \tag{40}$$

$$\boldsymbol{\sigma}_p^{(k)} = \mathbf{B}_1\mathbf{u}^{(k)} + \mathbf{B}_2u_3^{(k)} + \mathbf{B}_3\sigma_3^{(k-1)} + \mathbf{B}_4D_3^{(k)}, \tag{41}$$

$$\mathbf{d}^{(k)} = \mathbf{B}_5\boldsymbol{\sigma}_s^{(k)} + \mathbf{B}_6\phi^{(k)}. \tag{42}$$

The transverse loads and electric potential at the lateral surfaces are given as

Order $\in^0$:

$$[\tau_{13}^{(0)}\ \ \tau_{23}^{(0)}] = [0\ \ 0] \quad \text{on } x_3 = \pm 1, \tag{43a}$$

$$\sigma_3^{(0)} = \overline{q}_3^{\pm}(x_1, x_2) \quad \text{on } x_3 = \pm 1, \tag{43b}$$

$$\phi^{(0)} = \overline{\phi}^{\pm}(x_1, x_2) \quad \text{on } x_3 = \pm 1. \tag{44}$$

Order $\in^{2k}$ ($k = 1, 2, 3$, etc.):

$$[\tau_{13}^{(k)}\ \ \tau_{23}^{(k)}\ \ \sigma_3^{(k)}] = [0\ \ 0\ \ 0] \quad \text{on } x_3 = \pm 1, \tag{45}$$

$$\phi^{(k)} = 0 \quad \text{on } x_3 = \pm 1. \tag{46}$$

Along the edges one member of each pair of the following quantities must be satisfied:

Order $\in^0$:

$$n_1\sigma_1^{(0)} + n_2\tau_{12}^{(0)} = p_{n1} \quad \text{or} \quad u_1^{(0)} = \overline{u}_1, \tag{47a}$$

$$n_1\tau_{12}^{(0)} + n_2\sigma_2^{(0)} = p_{n2} \quad \text{or} \quad u_2^{(0)} = \overline{u}_2, \tag{47b}$$

$$n_1\tau_{13}^{(0)} + n_2\tau_{23}^{(0)} = p_{n3} \quad \text{or} \quad u_3^{(0)} = \overline{u}_3, \tag{47c}$$

$$\phi^{(0)} = 0. \tag{48}$$

Order $\in^{2k}$ ($k = 1, 2, 3$, etc.):

$$n_1\sigma_1^{(k)} + n_2\tau_{12}^{(k)} = 0 \quad \text{or} \quad u_1^{(k)} = 0, \tag{49a}$$

$$n_1\tau_{12}^{(k)} + n_2\sigma_2^{(k)} = 0 \quad \text{or} \quad u_2^{(k)} = 0, \tag{49b}$$

$$n_1\tau_{13}^{(k)} + n_2\tau_{23}^{(k)} = 0 \quad \text{or} \quad u_3^{(k)} = 0, \tag{49c}$$

$$\phi^{(k)} = 0. \tag{50}$$

5. Successive integration

5.1. Governing equations of the leading-order problem

Examination of the sets of asymptotic equations, it is found that the analysis can be carried on by integrating those equations through the thickness direction. We therefore integrate Eqs. (27)–(29) to obtain

$$u_3^{(0)} = u_3^0(x_1, x_2), \tag{51}$$

$$\mathbf{u}^{(0)} = \mathbf{u}^0 - x_3\mathbf{D}u_3^0, \tag{52}$$

$$D_3^{(0)} = D_3^0(x_1, x_2), \tag{53}$$

where $u_3^0(x_1, x_2)$, $\mathbf{u}^0 = [u_1^0(x_1, x_2)\ \ u_2^0(x_1, x_2)]^{\mathrm{T}}$ and $D_3^0(x_1, x_2)$ represent the displacements and piezoelectric displacement on the middle surface.

Using the lateral boundary conditions on $x_3 = -1$ (i.e., Eqs. (43)–(44)) and then successively integrating Eqs. (30)–(32) through the thickness, we obtain

$$\boldsymbol{\sigma}_s^{(0)} = -\int_{-1}^{x_3}[\mathbf{L}_5(\mathbf{u}^0 - \eta\mathbf{D}u_3^0) + \mathbf{L}_6u_3^0 + \mathbf{L}_8D_3^0]\,\mathrm{d}\eta, \tag{54}$$

$$\sigma_3^{(0)} = \overline{q}_3^- + \int_{-1}^{x_3}[\mathbf{L}_9(\mathbf{u}^0 - \eta\mathbf{D}u_3^0) + \tilde{l}_{63}u_3^0 + \tilde{l}_{65}D_3^0]\,\mathrm{d}\eta + \int_{-1}^{x_3}(x_3 - \eta)\mathbf{D}^{\mathrm{T}}[\mathbf{L}_5(\mathbf{u}^0 - \eta\mathbf{D}u_3^0) + \mathbf{L}_6u_3^0 + \mathbf{L}_8D_3^0]\,\mathrm{d}\eta, \tag{55}$$

$$\phi^{(0)} = \overline{\phi}^- - \int_{-1}^{x_3}[(1/\gamma_\theta)\mathbf{L}_8^{\mathrm{T}}(\mathbf{u}^0 - \eta\mathbf{D}u_3^0) + (1/\gamma_\theta)\tilde{l}_{65}u_3^0 + \tilde{l}_{81}D_3^0]\,\mathrm{d}\eta. \tag{56}$$

Imposition of the remaining lateral boundary conditions on $x_3 = 1$ (i.e., Eqs. (43)–(44)) in Eqs. (54)–(56) yields

$$K_{11}u_1^0 + K_{12}u_2^0 + K_{13}u_3^0 + K_{14}D_3^0 = 0, \tag{57}$$

$$K_{21}u_1^0 + K_{22}u_2^0 + K_{23}u_3^0 + K_{24}D_3^0 = 0, \tag{58}$$

$$K_{31}u_1^0 + K_{32}u_2^0 + K_{33}u_3^0 + K_{34}D_3^0 = \overline{q}_3^+ - \overline{q}_3^-, \tag{59}$$

$$K_{41}u_1^0 + K_{42}u_2^0 + K_{43}u_3^0 + K_{44}D_3^0 = \overline{\phi}^+ - \overline{\phi}^-, \tag{60}$$

in which

$$K_{11} = \hat{A}_{11}\partial_{11} + (\tilde{A}_{16} + \tilde{A}_{61})\partial_{12} + \overline{A}_{66}\partial_{22},$$

$$K_{12} = \hat{A}_{16}\partial_{11} + (\tilde{A}_{12} + \tilde{A}_{66})\partial_{12} + \overline{A}_{62}\partial_{22},$$

$$\begin{aligned} K_{13} = & -\hat{B}_{11}\partial_{111} - (\tilde{B}_{16} + \hat{B}_{16} + \tilde{B}_{61})\partial_{112} \\ & - (\tilde{B}_{12} + \tilde{B}_{66} + \overline{B}_{66})\partial_{122}, \\ & - \overline{B}_{62}\partial_{222} + \tilde{A}_{12}\partial_1 + \overline{A}_{62}\partial_2, \end{aligned}$$

$$K_{14} = \hat{E}_{31}\partial_1 + \tilde{E}_{36}\partial_2,$$

$$K_{21} = \hat{A}_{61}\partial_{11} + (\tilde{A}_{21} + \tilde{A}_{66})\partial_{12} + \overline{A}_{26}\partial_{22},$$

$$K_{22} = \hat{A}_{66}\partial_{11} + (\tilde{A}_{26} + \tilde{A}_{62})\partial_{12} + \overline{A}_{22}\partial_{22},$$

$$\begin{aligned} K_{23} = & -\hat{B}_{61}\partial_{111} - (\tilde{B}_{21} + \tilde{B}_{66} + \hat{B}_{66})\partial_{112} \\ & - (\overline{B}_{26} + \tilde{B}_{26} + \tilde{B}_{62})\partial_{122} \\ & - \overline{B}_{22}\partial_{222} + \tilde{A}_{62}\partial_1 + \overline{A}_{22}\partial_2, \end{aligned}$$

$$K_{24} = \hat{E}_{36}\partial_1 + \tilde{E}_{32}\partial_2,$$

$$\begin{aligned} K_{31} = & -\hat{B}_{11}\partial_{111} - (\tilde{B}_{16} + \tilde{B}_{61} + \hat{B}_{61})\partial_{112} \\ & - (\tilde{B}_{21} + \tilde{B}_{66} + \overline{B}_{66})\partial_{122} \\ & - \overline{B}_{26}\partial_{222} + \tilde{A}_{21}\partial_1 + \overline{A}_{26}\partial_2, \end{aligned}$$

$$\begin{aligned} K_{32} = & -\hat{B}_{16}\partial_{111} - (\tilde{B}_{12} + \tilde{B}_{66} + \hat{B}_{66})\partial_{112} \\ & - (\tilde{B}_{26} + \tilde{B}_{62} + \overline{B}_{62})\partial_{122} \\ & - \overline{B}_{22}\partial_{222} + \tilde{A}_{26}\partial_1 + \overline{A}_{22}\partial_2, \end{aligned}$$

$$\begin{aligned} K_{33} = & \hat{D}_{11}\partial_{1111} + (\tilde{D}_{16} + \hat{D}_{16} + \tilde{D}_{61} + \hat{D}_{61})\partial_{1112} \\ & + (\tilde{D}_{12} + \tilde{D}_{21} + \overline{D}_{66} + 2\tilde{D}_{66} + \hat{D}_{66})\partial_{1122} \\ & + (\overline{D}_{26} + \tilde{D}_{26} + \overline{D}_{62} + \tilde{D}_{62})\partial_{1222} + \overline{D}_{22}\partial_{2222} \\ & - (\tilde{B}_{12} + \tilde{B}_{21})\partial_{11} \\ & - (\overline{B}_{26} + \overline{B}_{62} + \tilde{B}_{26} + \tilde{B}_{62})\partial_{12} \\ & - 2\overline{B}_{22}\partial_{22} + \overline{A}_{22}, \end{aligned}$$

$$K_{34} = -\hat{F}_{31}\partial_{11} - (\hat{F}_{36} + \tilde{F}_{36})\partial_{12} - \tilde{F}_{32}\partial_{22} + \tilde{E}_{32},$$

$$K_{41} = -\tilde{E}_{31}\partial_1 - \overline{E}_{36}\partial_2,$$

$$K_{42} = -\tilde{E}_{36}\partial_1 - \overline{E}_{32}\partial_2,$$

$$K_{43} = \tilde{F}_{31}\partial_{11} + (\overline{F}_{36} + \tilde{F}_{36})\partial_{12} + \overline{F}_{32}\partial_{22} - \overline{E}_{32},$$

$$K_{44} = -E_0,$$

$$\hat{A}_{ij} = \int_{-1}^{1} (\tilde{Q}_{ij}\gamma_\theta)\,\mathrm{d}x_3, \quad \tilde{A}_{ij} = \int_{-1}^{1} \tilde{Q}_{ij}\,\mathrm{d}x_3,$$
$$\overline{A}_{ij} = \int_{-1}^{1} (\tilde{Q}_{ij}/\gamma_\theta)\,\mathrm{d}x_3,$$

$$\hat{B}_{ij} = \int_{-1}^{1} x_3(\tilde{Q}_{ij}\gamma_\theta)\,\mathrm{d}x_3, \quad \tilde{B}_{ij} = \int_{-1}^{1} x_3\tilde{Q}_{ij}\,\mathrm{d}x_3,$$
$$\overline{B}_{ij} = \int_{-1}^{1} x_3(\tilde{Q}_{ij}/\gamma_\theta)\,\mathrm{d}x_3,$$

$$\hat{D}_{ij} = \int_{-1}^{1} x_3^2(\tilde{Q}_{ij}\gamma_\theta)\,\mathrm{d}x_3, \quad \tilde{D}_{ij} = \int_{-1}^{1} x_3^2\tilde{Q}_{ij}\,\mathrm{d}x_3,$$
$$\overline{D}_{ij} = \int_{-1}^{1} x_3^2(\tilde{Q}_{ij}/\gamma_\theta)\,\mathrm{d}x_3,$$

$$(\hat{E}_{3i}\ \ \hat{F}_{3i}) = \int_{-1}^{1} (1\ \ x_3)\left(\frac{\gamma_\theta e}{Q}\right)\left(\frac{e_{33}c_{3i} - e_{3i}c_{33}}{e_{33}^2 + \eta_{33}c_{33}}\right)\mathrm{d}x_3,$$

$$(\tilde{E}_{3i}\ \ \tilde{F}_{3i}) = \int_{-1}^{1} (1\ \ x_3)\left(\frac{e}{Q}\right)\left(\frac{e_{33}c_{3i} - e_{3i}c_{33}}{e_{33}^2 + \eta_{33}c_{33}}\right)\mathrm{d}x_3,$$

$$(\overline{E}_{3i}\ \ \overline{F}_{3i}) = \int_{-1}^{1} (1\ \ x_3)\left(\frac{e}{\gamma_\theta Q}\right)\left(\frac{e_{33}c_{3i} - e_{3i}c_{33}}{e_{33}^2 + \eta_{33}c_{33}}\right)\mathrm{d}x_3,$$

$$E_0 = \int_{-1}^{1} \left(\frac{e^2}{Q}\right)\left(\frac{c_{33}}{e_{33}^2 + \eta_{33}c_{33}}\right)\mathrm{d}x_3.$$

Solution of Eqs. (57)–(60) must be supplemented with the edge boundary conditions Eqs. (47)–(48) to constitute a well-posed boundary value problem. Once u_1^0, u_2^0, u_3^0 and D_3^0 are determined, the leading-order solutions of displacements, transverse shear and normal stresses, in-surface stresses, in-surface electric displacements and electric potential can be obtained by Eqs. (51)–(53), (54)–(55), (33), (34) and (56), respectively.

5.2. Governing equations of higher-order problems

Proceed to order ϵ^{2k} ($k = 1, 2, 3$, etc.) following the same line as was done before, we readily obtain

$$u_3^{(k)} = u_3^k(x_1, x_2) + \varphi_{3k}(x_1, x_2, x_3), \tag{61}$$

$$\mathbf{u}^{(k)} = \mathbf{u}^k - x_3\mathbf{D}u_3^k + \boldsymbol{\varphi}^k, \tag{62}$$

$$D_3^{(k)} = D_3^k(x_1, x_2) + \varphi_{4k}(x_1, x_2, x_3), \tag{63}$$

$$\begin{aligned} \boldsymbol{\sigma}_s^{(k)} = & -\int_{-1}^{x_3} [\mathbf{L}_5(\mathbf{u}^k - \eta\mathbf{D}u_3^k) + \mathbf{L}_6u_3^k + \mathbf{L}_8D_3^k]\,\mathrm{d}\eta \\ & + \mathbf{f}^k(x_1, x_2, x_3), \end{aligned} \tag{64}$$

$$\sigma_3^{(k)} = \int_{-1}^{x_3} [\mathbf{L}_9(\mathbf{u}^k - \eta \mathbf{D} u_3^k) + \tilde{l}_{63} u_3^k + \tilde{l}_{65} D_3^k]\,\mathrm{d}\eta + \int_{-1}^{x_3} (x_3 - \eta)\mathbf{D}^{\mathrm{T}}[\mathbf{L}_5(\mathbf{u}^k - \eta \mathbf{D} u_3^k) + \mathbf{L}_6 u_3^k + \mathbf{L}_8 D_3^k]\,\mathrm{d}\eta - f_{3k}(x_1, x_2, x_3), \tag{65}$$

$$\phi^{(k)} = -\int_{-1}^{x_3} [(1/\gamma_\theta)\,\mathbf{L}_8^{\mathrm{T}}(\mathbf{u}^k - \eta \mathbf{D} u_3^k) + (1/\gamma_\theta)\,\tilde{l}_{65} u_3^k + \tilde{l}_{81} D_3^k]\,\mathrm{d}\eta - f_{4k}(x_1, x_2, x_3), \tag{66}$$

where

$$\varphi_{3k}(x_1, x_2, x_3) = -\int_0^{x_3} [\mathbf{L}_1 \mathbf{u}^{(k-1)} + \tilde{l}_{33} u_3^{(k-1)} - \tilde{l}_{35} D_3^{(k-1)} - \tilde{l}_{34} \sigma_3^{(k-2)}]\,\mathrm{d}\eta,$$

$$\mathbf{u}^k = [u_1^k(x_1, x_2) \quad u_2^k(x_1, x_2)]^{\mathrm{T}},$$

$$\boldsymbol{\varphi}^k = \begin{Bmatrix} \varphi_{1k}(x_1, x_2, x_3) \\ \varphi_{2k}(x_1, x_2, x_3) \end{Bmatrix} = -\int_0^{x_3} (\mathbf{D}\varphi_{3k} - \mathbf{L}_2 \mathbf{u}^{(k)} - \mathbf{S}\boldsymbol{\sigma}_s^{(k-1)} - \mathbf{L}_3 \boldsymbol{\sigma}_s^{(k-2)} - \mathbf{L}_4 \boldsymbol{\phi}^{(k-1)})\,\mathrm{d}\eta,$$

$$\varphi_{4k} = -\int_0^{x_3} (\mathbf{L}_{11} \mathbf{d}^{(k-1)} + \tilde{l}_{71} D_3^{(k-1)})\,\mathrm{d}\eta,$$

$$\mathbf{f}^k = -\int_{-1}^{x_3} [\mathbf{L}_5 \boldsymbol{\varphi}^k + \mathbf{L}_6 \varphi_{3k} + \mathbf{L}_8 \varphi_{4k} + \mathbf{L}_7 \boldsymbol{\sigma}_s^{(k-1)} + (\gamma_\theta)\mathbf{L}_1^{\mathrm{T}} \boldsymbol{\sigma}_3^{(k-1)}]\,\mathrm{d}\eta,$$

$$f_{3k} = -\int_{-1}^{x_3} [\mathbf{L}_9 \boldsymbol{\varphi}^k + \tilde{l}_{63} \varphi_{3k} - \mathbf{L}_{10} \boldsymbol{\sigma}_s^{(k-1)} - \tilde{l}_{64} \sigma_3^{(k-1)} + \tilde{l}_{65} \varphi_{4k} + \mathbf{D}^{\mathrm{T}} \mathbf{f}^k]\,\mathrm{d}\eta,$$

$$f_{4k} = \int_{-1}^{x_3} [(1/\gamma_\theta)\mathbf{L}_8^{\mathrm{T}} \boldsymbol{\phi}^k + (1/\gamma_\theta)\tilde{l}_{65} \varphi_{3k} - \tilde{l}_{35} \sigma_3^{(k-1)} - \tilde{l}_{81} \varphi_{4k}]\,\mathrm{d}\eta.$$

w^k, $\mathbf{u}^k$ and D_3^k represent the modifications to the elastic and electric displacements on the middle surface. Upon imposing the associated lateral boundary conditions Eqs. (45)–(46) on Eqs. (64) and (66), we arrive again at the CST-type equations, only with nonhomogeneous terms that can be calculated from the lower-order solution. The governing equations for $\in^{2k}$-order are given by

$$K_{11} u_1^k + K_{12} u_2^k + K_{13} u_3^k + K_{14} D_3^k = f_{1k}(x_1, x_2, 1), \tag{67}$$

$$K_{21} u_1^k + K_{22} u_2^k + K_{23} u_3^k + K_{24} D_3^k = f_{2k}(x_1, x_2, 1), \tag{68}$$

$$K_{31} u_1^k + K_{32} u_2^k + K_{33} u_3^k + K_{34} D_3^k = f_{3k}(x_1, x_2, 1) - \frac{\partial f_{1k}(x_1, x_2, 1)}{\partial x_1} - \frac{\partial f_{2k}(x_1, x_2, 1)}{\partial x_2}, \tag{69}$$

$$K_{41} u_1^k + K_{42} u_2^k + K_{43} u_3^k + K_{44} D_3^k = f_{4k}(x_1, x_2, 1). \tag{70}$$

Again, solution of Eqs. (67)–(70) must be supplemented with the edge boundary conditions Eqs. (49)–(50) to constitute a well-posed boundary value problem. Once u_1^k, u_2^k, u_3^k and D_3^k are determined, the high-order modifications of displacements, transverse shear and normal stresses, in-surface stresses, in-surface electric displacements and electric potential can be obtained by Eqs. (61)–(63), (64)–(65), (41), (42) and (66), respectively.

5.3. Supplementary remarks

As aforementioned, once the elastic and normal electric displacements on the middle surface at each order level are determined, the corresponding transverse stresses, normal electric displacement and electric potential can then be determined. These previously mentioned equations represent certain integrations integrating the relevant functions from the bottom surface to a certain position in the thickness direction. That leads to the continuous values of out-of-surface field variables through the thickness coordinate if there is no any electromechanical load applied at interfaces between layers. In addition, the lateral boundary conditions are regarded as the imposition conditions to obtain the governing equations for various orders and inherently be satisfied in the present analysis.

There are some researchers, such as Heyliger and Saravanos [18], Vel and Batra [19] and Sun and Zhang [20], concerned the analysis for shear actuated laminates where the piezoelectric layer is embedded in composite laminates and concentrated electric potentials are applied at the interfaces between the elastic and electric layers. In that cases of shear actuated laminates the present formulation need to be minor modified and make additional remarks as follows.

Consider an actuated laminate where a piezoelectric layer is embedded as the jth layer in the laminate and the thickness coordinates of the bottom and top surfaces of the piezoelectric layer are $x_3 = z_{j-1}$ and $x_3 = z_j$, respectively. The electric potentials $\overline{\phi}_j^-$ and $\overline{\phi}_j^+$ are applied at the bottom and top surfaces of the piezoelectric layer, respectively. The shear actuated conditions can be written as

Order $\in^0$:

$$\phi^{(0)}(z_{j-1}^+) - \phi^{(0)}(z_{j-1}^-) = \overline{\phi}_j^-, \tag{71}$$

$$\phi^{(0)}(z_j^+) - \phi^{(0)}(z_j^-) = -\overline{\phi}_j^+. \tag{72}$$

Order $\in^{2k}$ ($k = 1, 2, 3$, etc.):

$$\phi^{(k)}(z_{j-1}^+) - \phi^{(k)}(z_{j-1}^-) = 0, \tag{73}$$

$$\phi^{(k)}(z_j^+) - \phi^{(k)}(z_j^-) = 0. \tag{74}$$

On the basis of previous interfacial conditions, we realize that only the fourth governing equation of the leading order is needed to be remedied. Let us reexamine Eq. (56) and rewrite it to account for these interfacial

conditions as follows:

$$\begin{aligned}\overline{\phi}^{+} &= \overline{\phi}^{-} - \int_{-1}^{1}[(1/\gamma_\theta)\,\mathbf{L}_8^{\mathrm{T}}(\mathbf{u}^0 - \eta\,\mathbf{D}\,u_3^0) \\ &\quad + (1/\gamma_\theta)\,\tilde{l}_{65}u_3^0 + \tilde{l}_{81}D_3^0]\,\mathrm{d}\eta \\ &= \overline{\phi}^{-} - \int_{-1}^{z_{j-1}^{-}}[\cdots]\,\mathrm{d}\eta - \overline{\phi}_j^{-} - \int_{z_{j-1}^{+}}^{z_j^{-}}[\cdots]\,\mathrm{d}\eta \\ &\quad + \overline{\phi}_j^{+} - \int_{z_j^{+}}^{1}[\cdots]\,\mathrm{d}\eta. \end{aligned} \tag{75}$$

After a rearrangement of Eq. (75), we may obtain the modified fourth governing of the leading-order and given by

$$K_{41}u_1^0 + K_{42}u_2^0 + K_{43}u_3^0 + K_{44}D_3^0 = \overline{\phi}^{+} - \overline{\phi}^{-} + \overline{\phi}_j^{+} - \overline{\phi}_j^{-}. \tag{76}$$

Once the elastic and normal electric displacements are determined, we may use the aforementioned equations to calculate the through-thickness distributions of these out-of-surface field variables, Since the shear actuated conditions are applied at the interfaces between the elastic and embedded piezoelectric layers, the variable of electric potential will exist a jump at these interfaces. The other out-of-surface field variables may reveal the similar jumping situation at the interfaces if the corresponding integrations involve a mathematic calculation with respect to the electric potential.

6. Applications to benchmark problems

The benchmark problems of simply supported, single-layer and multilayered piezoelectric hollow cylinders under mechanical or electric loads on outer surfaces are studied using the present asymptotic formulation. The cylinders composed of the orthotropic elastic and piezoelectric layers are considered so that the following elastic and electric moduli are identical zero,

$$(Q_{16})_i = (Q_{26})_i = (Q_{36})_i = (Q_{45})_i = 0, \tag{77a}$$

$$(e_{14})_i = (e_{25})_i = (e_{36})_i = (\eta_{12})_i = 0. \tag{77b}$$

The boundary conditions at edges are of a shear diaphragm type specified by

$$\sigma_1 = u_2 = u_3 = \Phi = 0 \quad \text{on } x_1 = 0 \text{ and } x_1 = L/R \in . \tag{78}$$

The mechanical or electric loads acting on lateral surface of the shell ($\zeta = h$) are considered in the following illustrated examples and are expressed by the double Fourier series in the dimensionless form

$$\tilde{q}(x_1, x_2) = \sum_{m=1}^{\infty}\sum_{n=0}^{\infty}\tilde{q}_{mn}\sin\,\tilde{m}x_1\cos\tilde{n}x_2, \tag{79}$$

$$\tilde{\phi}(x_1, x_2) = \sum_{m=1}^{\infty}\sum_{n=0}^{\infty}\tilde{\phi}_{mn}\sin\tilde{m}x_1\cos\tilde{n}x_2, \tag{80}$$

where $\tilde{m} = m\pi\sqrt{Rh}/L$ and $\tilde{n} = n\sqrt{h/R}$.

The governing equations of the leading-order problem (Eqs. (57)–(60)) can be readily solved by letting

$$u_1^0 = \sum_{m=1}^{\infty}\sum_{n=0}^{\infty}u_{1mn}^0\cos\tilde{m}x_1\,\cos\tilde{n}x_2, \tag{81}$$

$$u_2^0 = \sum_{m=1}^{\infty}\sum_{n=0}^{\infty}u_{2mn}^0\sin\tilde{m}x_1\sin\tilde{n}x_2, \tag{82}$$

$$u_3^0 = \sum_{m=1}^{\infty}\sum_{n=0}^{\infty}u_{3mn}^0\sin\tilde{m}x_1\cos\tilde{n}x_2, \tag{83}$$

$$D_3^0 = \sum_{m=1}^{\infty}\sum_{n=0}^{\infty}D_{3mn}^0\sin\tilde{m}x_1\cos\tilde{n}x_2. \tag{84}$$

Substituting Eqs. (81)–(84) into Eqs. (57)–(60)) gives

$$\begin{bmatrix} k_{11} & k_{12} & k_{13} & k_{14} \\ k_{21} & k_{22} & k_{23} & k_{24} \\ k_{31} & k_{32} & k_{33} & k_{34} \\ k_{41} & k_{42} & k_{43} & k_{44} \end{bmatrix}\begin{Bmatrix} u_{1mn}^0 \\ u_{2mn}^0 \\ u_{3mn}^0 \\ D_{3mn}^0 \end{Bmatrix} = \begin{Bmatrix} 0 \\ 0 \\ \tilde{q}_{mn} \\ \tilde{\phi}_{mn} \end{Bmatrix}, \tag{85}$$

where k_{ij} are the relative coefficients.

u_{1mn}^0, u_{2mn}^0 and u_{3mn}^0 can be obtained by solving the simultaneously algebraic equations (85). Once u_{1mn}^0, u_{2mn}^0 and u_{3mn}^0 are determined, the ϵ^0-order solution can be obtained as aforementioned. The summation signs would be dropped for brevity in the following derivation.

Carrying on the solution to order ϵ^2, we find that the nonhomogeneous terms for fixed values of m and n in the ϵ^2-order equations are

$$f_{11}(x_1, x_2, 1) = \tilde{f}_{11}(1)\cos\tilde{m}x_1\cos\tilde{n}x_2, \tag{86}$$

$$f_{21}(x_1, x_2, 1) = \tilde{f}_{21}(1)\sin\tilde{m}x_1\sin\tilde{n}x_2, \tag{87}$$

$$f_{31}(x_1, x_2, 1) = \tilde{f}_{31}(1)\sin\tilde{m}x_1\cos\tilde{n}x_2, \tag{88}$$

$$f_{41}(x_1, x_2, 1) = \tilde{f}_{41}(1)\sin\tilde{m}x_1\cos\tilde{n}x_2. \tag{89}$$

In view of the recurrence of the equations, the ϵ^2-order solution can be obtained by letting

$$u_1^1 = u_{1mn}^1\cos\tilde{m}x_1\cos\tilde{n}x_2, \tag{90}$$

$$u_2^1 = u_{2mn}^1\sin\tilde{m}x_1\sin\tilde{n}x_2, \tag{91}$$

$$u_3^1 = u_{3mn}^1\sin\tilde{m}x_1\cos\tilde{n}x_2, \tag{92}$$

$$D_3^1 = D_{3mn}^1\sin\tilde{m}x_1\cos\tilde{n}x_2, \tag{93}$$

Substituting Eqs. (90)–(93) into Eqs. (67)–(70) gives

$$\begin{bmatrix} k_{11} & k_{12} & k_{13} & k_{14} \\ k_{21} & k_{22} & k_{23} & k_{24} \\ k_{31} & k_{32} & k_{33} & k_{34} \\ k_{41} & k_{42} & k_{43} & k_{44} \end{bmatrix} \begin{Bmatrix} u^1_{1mn} \\ u^1_{2mn} \\ u^1_{3mn} \\ D^1_{3mn} \end{Bmatrix} = \begin{Bmatrix} \tilde{f}_{11}(1) \\ \tilde{f}_{21}(1) \\ \tilde{f}_{31}(1) - \tilde{m}\tilde{f}_{11}(1) + \tilde{n}\tilde{f}_{21}(1) \\ \tilde{f}_{41}(1) \end{Bmatrix}, \tag{94}$$

u^1_{1mn}, u^1_{2mn}, u^1_{3mn} and D^1_{3mn} are easily obtained by solving the system of algebraic equations (94). Afterwards, the ϵ^2-order corrections are determined from Eqs. (61)–(66) and (41)–(42).

Examining Eqs. (57)–(60) and (67)–(70), we find that the solutions are in recurrent forms. The higher-order corrections can be determined using the lower-order solutions in a hierarchic manner. Several benchmark solutions are calculated in the following examples using the present asymptotic formulation.

6.1. Single-layer axisymmetric piezoelectric hollow cylinders

For comparison purpose, the present 3D solutions of simply-supported, single-layer piezoelectric hollow cylinders under axisymmetric mechanical or electrical loads are computed and are compared with the accurate solutions in the literature [12]. The asymptotic formulation for axisymmetric piezoelectric cylinders can be obtained by letting the circumferential wave number (n) be zero in the present one. Either mechanical or electrical loads (i.e., $\overline{q}_r^+ = q_0 \sin \pi x/L$, $q_0 = -1\,\mathrm{N/m^2}$ or $\overline{\Phi}^+ = \phi_0 \sin \pi x/L$, $\phi_0 = 1\,\mathrm{V}$) on the lateral surface ($x_3 = 1$) is considered. The cylinders are considered to be composed of polyvinyledene fluoride (PVDF) polarized along the radial direction. The elastic, piezoelectric and dielectric properties of piezoelectric material are given in Table 1. The dimensionless variables are denoted as the same forms of those in Ref. [12] and given as follows.

In the cases of applied mechanical loads:

$$(\overline{u}_x, \overline{u}_r) = (u_x/2h, u_r/2h)/(|q_0|S^2/E_T),$$

$$(\overline{D}_x, \overline{D}_r) = (10D_xS/|q_0||d_T|, D_r/|q_0|S|d_T|),$$

$$(\overline{\sigma}_x, \overline{\sigma}_\theta, \overline{\sigma}_r, \overline{\tau}_{xr}) = (\sigma_x,\ \sigma_\theta/S,\ \sigma_r, \tau_{xr}S)/|q_0|,$$

$$\overline{\phi} = 1000\phi E_T|d_T|/2h|q_0|. \tag{95a–d}$$

In the cases of applied electrical potentials:

$$(\overline{u}_x,\ \overline{u}_r) = (u_x/\phi_0 S|d_T|,\ u_r/\phi_0 S|d_T|),$$

$$(\overline{D}_x,\ \overline{D}_r) = (2hD_xS/100\phi_0 E_T|d_T|^2,\ 2hD_r/\phi_0 E_T|d_T|^2),$$

$$(\overline{\sigma}_x,\ \overline{\sigma}_\theta) = (2hS\sigma_x/\phi_0 E_T|d_T|,\quad 2hS\sigma_\theta/\phi_0 E_T|d_T|),$$

$$(\overline{\sigma}_r,\ \overline{\tau}_{xr}) = (2hS^2\sigma_r/\phi_0 E_T|d_T|,\quad 20hS^2\tau_{xr}/\phi_0 E_T|d_T|),$$

$$\overline{\phi} = \phi/\phi_0, \tag{96a–e}$$

and $S = R/2h$, $E_T = 2.0\,\mathrm{GPa}$, $|d_T| = 30 \times 10^{-12} C/N$.

Tables 2 and 3 show the present asymptotic solutions of elastic and electric field variables for various orders at crucial positions of the cylinders under lateral loads and lateral potentials, respectively. The asymptotic solutions are computed up to the ϵ^{16}-order level in order to closely examine the convergence of the present asymptotic solutions. It is shown that the convergent solutions are obtained at the ϵ^2-order level in the cases of thin shells

Table 1
Elastic, piezoelectric and dielectric properties of composite and piezoelectric materials

Moduli	PVDT [12]	Graphite/Epoxy [22]	PZT-4 [22]	Ceramics [23]	PZT-4 [23]
c_{11} (Gpa)	3.0	183.433	138.499	138.28	139.02
c_{22}	3.0	11.662	138.499	138.28	139.02
c_{33}	3.0	11.662	114.745	128.07	115.45
c_{12}	1.5	4.363	77.371	32.359	77.848
c_{13}	1.5	4.363	73.643	27.821	74.328
c_{23}	1.5	3.918	73.643	27.821	74.328
c_{44}	0.75	2.870	25.6	53.5	25.6
c_{55}	0.75	7.170	25.6	53.5	25.6
c_{66}	0.75	7.170	30.6	53.0	30.6
e_{24} (C/m^2)	0.0	0.000	12.72	2.96	12.72
e_{15}	0.0	0.000	12.72	2.96	12.72
e_{31}	−0.15e−02	0.000	−5.2	0.8	−5.2
e_{32}	0.285e−01	0.000	−5.2	0.8	−5.2
e_{33}	−0.51e−01	0.000	15.08	6.88	15.08
η_{11} (F/m)	0.1062e−09	1.53e−08	1.306e−08	1.7885e−09	1.306e−08
η_{22}	0.1062e−09	1.53e−08	1.306e−08	1.7885e−09	1.306e−08
η_{33}	0.1062e−09	1.53e−08	1.151e−08	1.60257e−09	1.151e−08

Table 2
The elastic and electric field variables at crucial positions of single-layer piezoelectric hollow cylinders under lateral load

$R/2h$	$\in^{2k}$	$-\overline{U}_x(0,+h)$	$-\overline{U}_x(0,-h)$	$-\overline{U}_r(\frac{L}{2},+h)$	$-\overline{U}_r(\frac{L}{2},-h)$	$-\overline{D}_r(\frac{L}{2},+h)$	$-\overline{D}_r(\frac{L}{2},-h)$	$-\overline{\sigma}_x(\frac{L}{2},+h)$	$-\overline{\sigma}_x(\frac{L}{2},-h)$	$-\overline{\sigma}_\theta(\frac{L}{2},+h)$	$-\overline{\sigma}_\theta(\frac{L}{2},-h)$	$-\overline{\tau}_{xr}(0,0)$	$-\overline{\sigma}_r(\frac{L}{2},0)$	$-\overline{\phi}(\frac{L}{2},0)$
4	$\in^0$	0.3284	0.5237	0.9943	0.9943	0.7657	0.7657	0.1630	−0.1437	0.896	1.126	0.0304	0.5283	1.380
	$\in^2$	0.4326	0.6426	1.0328	1.1159	0.6382	0.8312	0.3455	−0.3549	1.029	1.247	0.0687	0.5893	1.693
	$\in^4$	0.4376	0.6458	1.0454	1.1062	0.6357	0.8210	0.3453	−0.3831	1.040	1.234	0.0712	0.5862	1.588
	$\in^6$	0.4373	0.6455	1.0467	1.1049	0.6373	0.8199	0.3479	−0.3843	1.042	1.232	0.0713	0.5859	1.580
	$\in^{16}$	0.4373	0.6455	1.0466	1.1049	0.6372	0.8200	0.3478	−0.3842	1.042	1.232	0.0712	0.5859	1.581
	3D solutions [21]	0.4373	0.6455	1.0466	1.1049	0.6372	0.8200	0.3478	−0.3842	1.042	1.232	0.0712	0.5859	1.581
10	$\in^0$	0.3854	0.4639	0.9991	0.9991	0.7665	0.7665	0.1604	−0.1529	0.9565	1.047	0.0308	0.5113	1.374
	$\in^2$	0.4275	0.5085	1.0152	1.0486	0.7162	0.7929	0.3463	−0.3508	1.011	1.093	0.0684	0.5351	1.628
	$\in^4$	0.4282	0.5091	1.0172	1.0471	0.7158	0.7914	0.3469	−0.3622	1.013	1.091	0.0696	0.5346	1.588
	$\in^6$	0.4282	0.5091	1.0173	1.0470	0.7159	0.7913	0.3473	−0.3623	1.013	1.091	0.0696	0.5346	1.587
	$\in^{16}$	0.4282	0.5091	1.0173	1.0470	0.7159	0.7913	0.3473	−0.3623	1.013	1.091	0.0696	0.5346	1.587
	3D solutions [21]	0.4282	0.5091	1.0173	1.0470	0.7159	0.7913	0.3473	−0.3623	1.013	1.091	0.0696	0.5346	1.587
100	$\in^0$	0.4205	0.4283	1.0000	1.0000	0.7667	0.7667	0.1576	−0.1569	0.996	1.005	0.0309	0.5011	1.373
	$\in^2$	0.4247	0.4326	1.0017	1.0050	0.7617	0.7693	0.3447	−0.3452	1.001	1.009	0.0677	0.5035	1.587
	$\in^4$	0.4247	0.4326	1.0017	1.0050	0.7617	0.7693	0.3448	−0.3463	1.001	1.009	0.0679	0.5035	1.584
	$\in^6$	0.4247	0.4326	1.0017	1.0050	0.7617	0.7693	0.3448	−0.3463	1.001	1.009	0.0679	0.5035	1.584
	$\in^{16}$	0.4247	0.4326	1.0017	1.0050	0.7617	0.7693	0.3448	−0.3463	1.001	1.009	0.0679	0.5035	1.584
	3D solutions [21]	0.4247	0.4326	1.002	1.005	0.7617	0.7693	0.3448	−0.3463	1.001	1.009	0.0679	0.5035	1.584

Table 3
The elastic and electric field variables at crucial positions of single-layer piezoelectric hollow cylinders under lateral potential

$R/2h$	$\in^{2k}$	$-\overline{U}_x(0,+h)$	$-\overline{U}_x(0,-h)$	$-\overline{U}_r(\frac{L}{2},+h)$	$-\overline{U}_r(\frac{L}{2},-h)$	$-\overline{D}_r(\frac{L}{2},+h)$	$-\overline{D}_r(\frac{L}{2},-h)$	$-\overline{\sigma}_x(\frac{L}{2},+h)$	$-\overline{\sigma}_x(\frac{L}{2},-h)$	$-\overline{\sigma}_\theta(\frac{L}{2},+h)$	$-\overline{\sigma}_\theta(\frac{L}{2},-h)$	$-\overline{\tau}_{xr}(0,0)$	$-\overline{\sigma}_r(\frac{L}{2},0)$	$-\overline{\phi}(\frac{L}{2},0)$
4	$\in^0$	0.2009	0.0512	−0.7623	−0.7623	−60.21	−60.21	−0.1250	0.1102	0.3175	−0.3851	−0.2327	−0.0868	0.500
	$\in^2$	0.1944	0.0466	−0.6317	−0.8816	−53.72	−67.71	−0.0997	0.1205	0.4608	−0.5465	−0.2178	−0.1241	0.529
	$\in^4$	0.1938	0.0460	−0.6370	−0.8860	−53.99	−68.02	−0.0971	0.1232	0.4569	−0.5501	−0.2157	−0.1240	0.529
	$\in^6$	0.1938	0.0460	−0.6372	−0.8858	−53.99	−68.02	−0.0974	0.1235	0.4562	−0.5490	−0.2158	−0.1238	0.528
	$\in^{16}$	0.1938	0.0460	−0.6372	−0.8858	−53.99	−68.02	−0.0974	0.1235	0.4562	−0.5490	−0.2158	−0.1238	0.528
	3D solutions [21]	0.1938	0.0460	−0.6372	−0.8858	−53.49	−68.02	−0.0974	0.1235	0.4562	−0.5490	−0.2158	−0.1238	0.528
10	$\in^0$	0.1572	0.0970	−0.7660	−0.7660	−60.21	−60.21	−0.1230	0.1172	0.3338	−0.3605	−0.2361	−0.0866	0.500
	$\in^2$	0.1562	0.0962	−0.7151	−0.8151	−57.37	−63.21	−0.1208	0.1297	0.4587	−0.4920	−0.2462	−0.1186	0.512
	$\in^4$	0.1561	0.0961	−0.7159	−0.8158	−57.42	−63.26	−0.1198	0.1307	0.4571	−0.4935	−0.2458	−0.1185	0.512
	$\in^6$	0.1561	0.0961	−0.7159	−0.8158	−57.42	−63.26	−0.1198	0.1308	0.4570	−0.4934	−0.2458	−0.1185	0.512
	$\in^{16}$	0.1561	0.0961	−0.7159	−0.8158	−57.42	−63.26	−0.1198	0.1308	0.4570	−0.4934	−0.2458	−0.1185	0.512
	3D solutions [21]	0.1561	0.0961	−0.7159	−0.8158	−57.42	−63.28	−0.1198	0.1308	0.4570	−0.4934	−0.2458	−0.1185	0.512
100	$\in^0$	0.1303	0.1243	−0.7667	−0.7667	−60.21	−60.21	−0.1209	0.1203	0.3450	−0.3477	−0.2368	−0.0866	0.500
	$\in^2$	0.1303	0.1243	−0.7617	−0.7717	−59.91	−60.51	−0.1314	0.1323	0.4599	−0.4632	−0.2590	−0.1154	0.501
	$\in^4$	0.1303	0.1243	−0.7617	−0.7717	−59.91	−60.51	−0.1313	0.1324	0.4597	−0.4634	−0.2590	−0.1154	0.501
	$\in^6$	0.1303	0.1243	−0.7617	−0.7717	−59.91	−60.51	−0.1313	0.1324	0.4597	−0.4634	−0.2590	−0.1154	0.501
	$\in^{16}$	0.1303	0.1243	−0.7617	−0.7717	−59.91	−60.51	−0.1313	0.1324	0.4597	−0.4634	−0.2590	−0.1154	0.501
	3D solutions [21]	0.1303	0.1243	−0.7617	−0.7717	−59.91	−60.51	−0.1313	0.1324	0.4597	−0.4634	−0.2590	−0.1154	0.501

($R/2h = 100$), at the ϵ^4-order level in the cases of moderately thick shells ($R/2h = 10$) and at the ϵ^6-order level in the cases of thick shells ($R/2h = 4$). The convergent solutions are also compared with the 3D piezoelectricity solutions available in the literature [21]. It is shown that the convergent solutions of the present asymptotic theory are in excellent agreement with the 3D piezoelectricity solutions.

Figs. 2 and 3 illustrate the variations of transverse stresses and electrical potentials through the thickness of the cylinder under lateral loads and lateral potentials, respectively. The geometric parameters of the cylinder are $R/2h = 10$ and $L/R = 4$. It is shown that the distribution of the transverse shear stress across the thickness is approximately parabolic and the maximum value occurs in the vicinity of the middle surface in the cases of applied lateral loads and lateral potentials. The distribution of the transverse normal stress through the thickness is approximately linear in the applied load case and approximately parabolic in the applied potential case. On the contrary, the distribution of the electric potential through the thickness is approximately parabolic in the applied load case and approximately linear in the applied potential case.

6.2. Single-layer nonaxisymmetric piezoelectric hollow cylinders

The single-layer piezoelectric hollow cylinders under applied mechanical or electrical loads (i.e., $\overline{q}_r^+ = q_0 \sin(\pi x/L)\cos 4\theta, q_0 = -1\,\mathrm{N/m^2}$ or $\overline{\Phi}^+ = \phi_0 \sin(\pi x/L)\cos 4\theta$, $\phi_0 = 1\,\mathrm{V}$) are considered. Piezoelectric material of PZT-4 [22] is used and its material properties are given in Table 1. The mechanical and electrical field variables are nondimensionalized as follows:

For the applied load cases,

$$\overline{u}_i = u_i c^*/q_0(2h), \quad \overline{\tau}_{ij} = \tau_{ij}/q_0, \quad \overline{\Phi} = \Phi e^*/q_0(2h), \quad \overline{D}_i = D_i c^*/q_0 e^*. \tag{97}$$

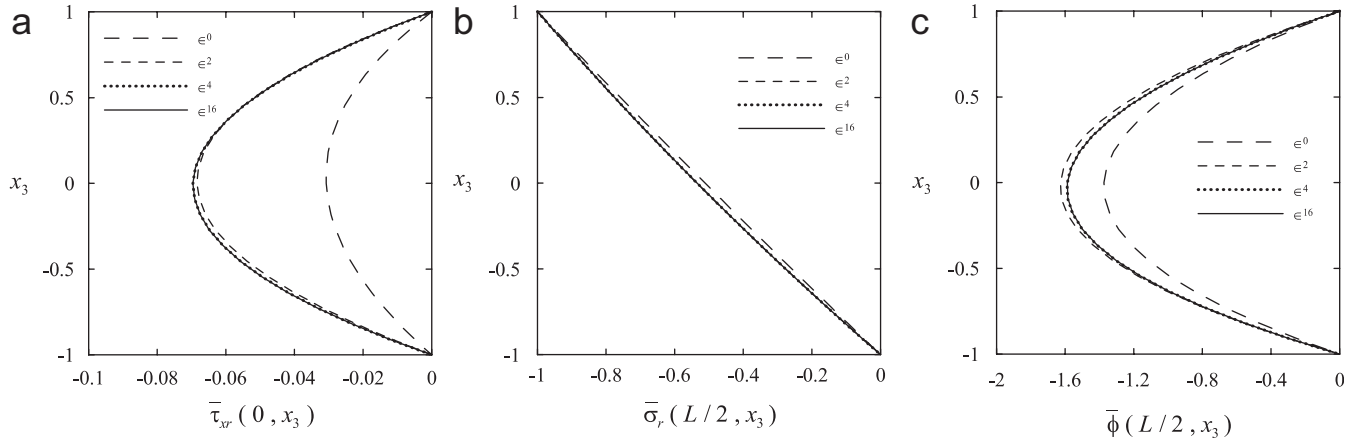

Fig. 2. The distributions of transverse stresses and electric potential through the thickness of a single-layer piezoelectric hollow cylinder under axisymmetric mechanical load.

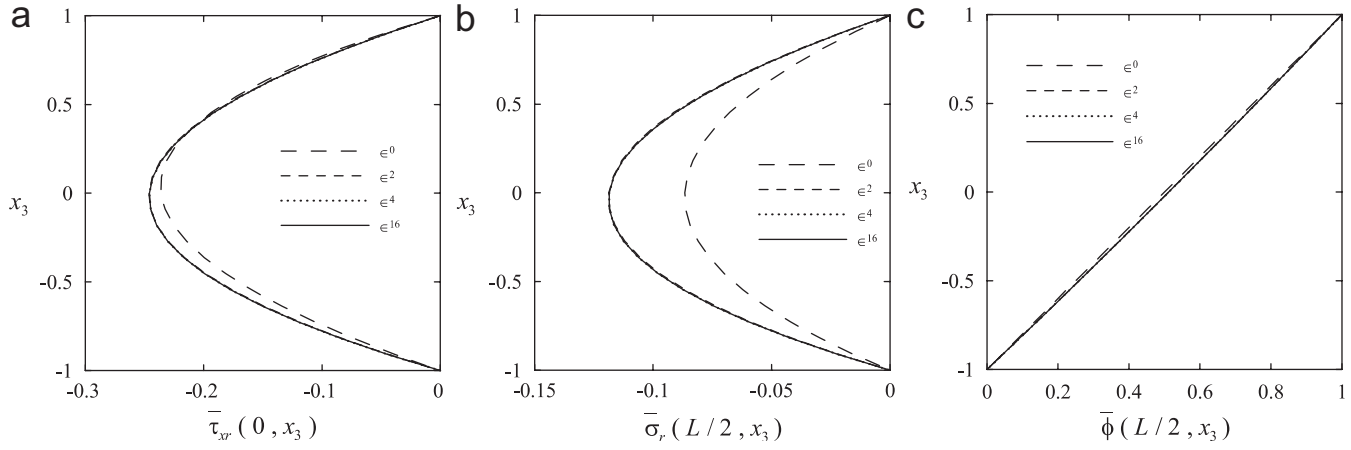

Fig. 3. The distributions of transverse stresses and electric potential through the thickness of a single-layer piezoelectric hollow cylinder under axisymmetric electric potential.

For the applied potential cases,

$$\overline{u}_i = u_i c^*/\phi_0 e^*, \quad \overline{\tau}_{ij} = \tau_{ij}(2h)/\phi_0 e^*, \quad \overline{\Phi} = \Phi/\phi_0,$$
$$\overline{D}_i = D_i c^*(2h)/\phi_0 (e^*)^2; \tag{98}$$

where $c^* = 1\,\mathrm{N/m^2}$, $e^* = 1\,\mathrm{C/m^2}$.

The distributions of present convergent solutions of various field variables for the applied potential cases with three different values of radius-to-thickness ratio S ($S = R/2h$) are shown in Fig. 4. It is noted that the distributions of the elastic displacement, stress and electric displacement through the thickness are highly nonlinear in the cases of thick shells under applied potentials. These results do not coincide with the basic assumptions of CST. That may cause unexpected errors in the piezoelectric analysis using CST for the moderately and thick shells. The distributions of field variables through the thickness in the cases of thick shells under lateral potentials change more dramatic than those under lateral loads. Hence, the advanced shell theory used for the piezoelectric analysis is more necessary than that used for the elastic analysis.

6.3. Multilayered hybrid piezoelectric plates

Since there are very few 3D solutions of multilayered piezoelectric cylinders available in the literature, the 3D solutions of multilayered piezoelectric plates under cylindrical bending presented by Heyliger and Brooks [23] are used to validate the present asymptotic solutions of multilayered piezoelectric laminates. Since the cylindrical coordinates system is adopted to develop the present asymptotic formulation, this formulation is suitable for both open-type cylindrical piezoelectric shells and piezoelectric cylinders. When the formulation is applied to the static analysis of open-type piezoelectric cylindrical shells, the excitations on the lateral surfaces of the shells will be expanded as double Fourier sine series

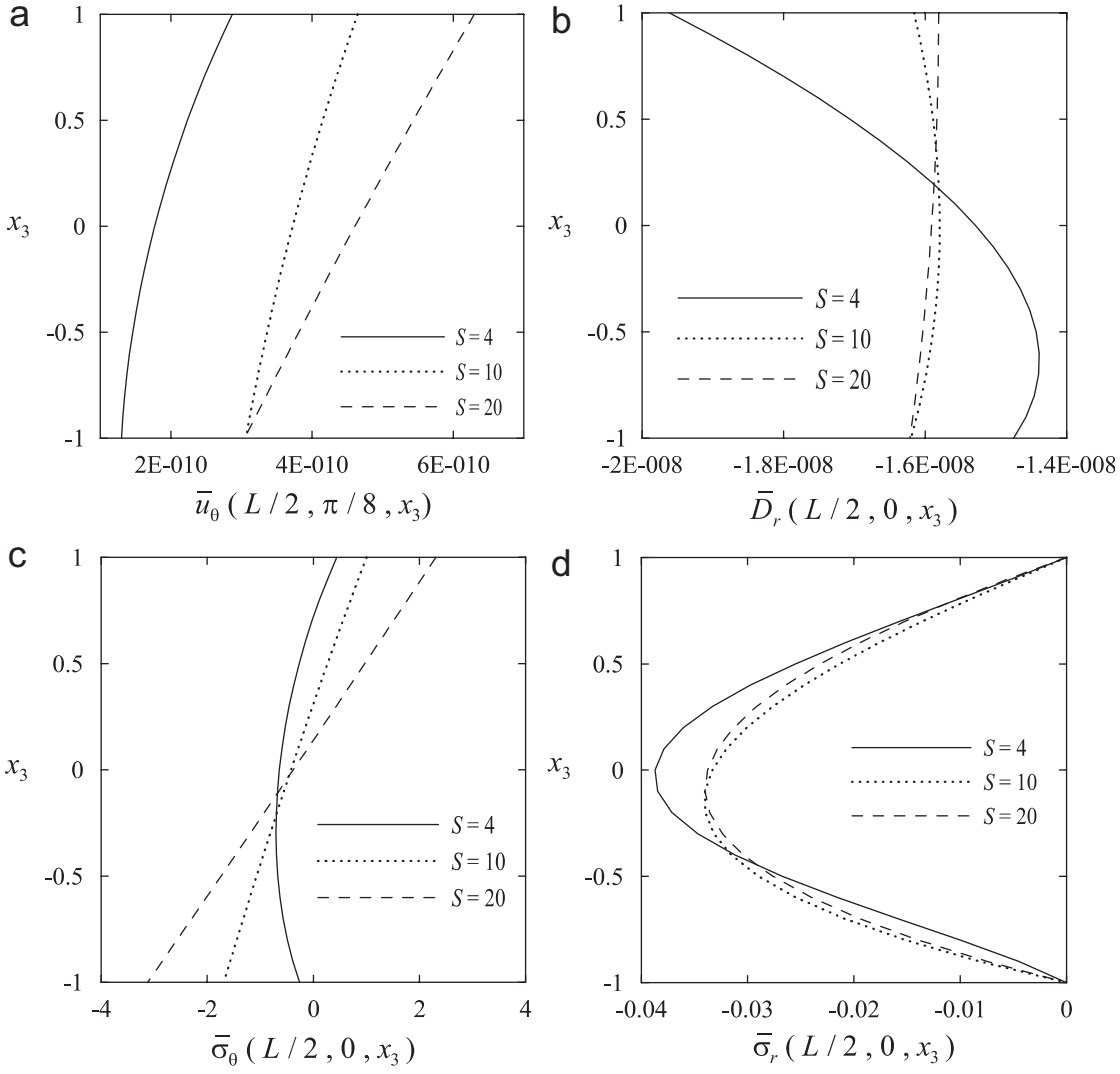

Fig. 4. The distributions of in-surface displacement and stress, transverse normal stress and normal electric displacement through the thickness of a single-layer piezoelectric hollow cylinder under electric potential for various ratios of radius-to-thickness.

Table 4
The elastic and electric field variables in a two-layer piezoelectric plate under cylindrical bending type of mechanical load

ζ	ϵ^{2k}	$\overline{v}(0,\zeta)\times 10^{13}$	$\overline{w}(\frac{L}{2},\zeta)\times 10^{10}$	$\overline{\phi}(\frac{L}{2},\zeta)\times 10^{4}$	$\overline{\sigma}_y(\frac{L}{2},\zeta)$	$\overline{\tau}_{yz}(0,\zeta)$	$\overline{\sigma}_z(\frac{L}{2},\zeta)$	$\overline{D}_z(\frac{L}{2},\zeta)\times 10^{10}$
h	ϵ^0	−172.421	1.03898	0.00000	57.8667	0.00000	1.000000	−4.05135
	ϵ^2	−170.397	1.05567	0.00000	57.8834	0.00000	1.000000	−2.22403
	ϵ^4	−170.415	1.05613	0.00000	57.8905	0.00000	1.000000	−2.21648
	ϵ^6	−170.415	1.05613	0.00000	57.8904	0.00000	1.000000	−2.21653
	ϵ^8	−170.415	1.05613	0.00000	57.8904	0.00000	1.000000	−2.21653
	Heyliger [23]	−170.406	1.05609	0.00000	57.8914	0.00000	1.000000	−2.21625
$\frac{1}{2}h$	ϵ^0	−90.8202	1.03898	10.6819	30.2683	3.46106	0.849898	−4.05135
	ϵ^2	−88.8919	1.06093	10.5712	30.1915	3.45455	0.850109	−2.68621
	ϵ^4	−88.8861	1.06109	10.5729	30.1903	3.45473	0.850097	−2.68009
	ϵ^6	−88.8861	1.06109	10.5729	30.1903	3.45473	0.850098	−2.68015
	ϵ^8	−88.8861	1.06109	10.5729	30.1903	3.45473	0.850098	−2.68015
	Heyliger [23]	−88.8804	1.06105	10.5763	30.1904	3.45477	0.850095	−2.67988
$0^{\pm}$	ϵ^0	−9.21893	1.03898	14.2755	2.66986 (3.69425)	4.75453	0.513086	−4.05135
	ϵ^2	−9.14274	1.06299	14.0648	2.93531 (3.77544)	4.75388	0.513757	−3.73478
	ϵ^4	−9.13397	1.06295	14.0663	2.93274 (3.77194)	4.75387	0.513739	−3.73426
	ϵ^6	−9.13402	1.06295	14.0662	2.93275 (3.77196)	4.75387	0.513739	−3.73427
	ϵ^8	−9.13402	1.06295	14.0662	2.93275 (3.77196)	4.75387	0.513739	−3.73427
	Heyliger [23]	−9.13120	1.06291	14.0706	2.93185 (3.77076)	4.75387	0.513734	−3.73402
$-\frac{1}{2}h$	ϵ^0	72.3823	1.03898	8.26632	−30.2683	3.71097	0.163188	−4.05135
	ϵ^2	72.3121	1.06277	8.14274	−30.2004	3.71727	0.163635	−3.87317
	ϵ^4	72.3128	1.06267	8.14370	−30.2007	3.71709	0.163625	−3.87360
	ϵ^6	72.3128	1.06267	8.14370	−30.2007	3.71709	0.163625	−3.87361
	ϵ^8	72.3128	1.06267	8.14370	−30.2007	3.71709	0.163625	−3.87361
	Heyliger [23]	72.3126	1.06263	8.14620	−30.2007	3.71705	0.163623	−3.87336
$-h$	ϵ^0	153.984	1.03898	0.00000	−64.2309	0.00000	0.00000	−4.05135
	ϵ^2	154.780	1.06129	0.00000	−64.5585	0.00000	0.00000	−3.94264
	ϵ^4	154.769	1.06116	0.00000	−64.5537	0.00000	0.00000	−3.94362
	ϵ^6	154.769	1.06116	0.00000	−64.5538	0.00000	0.00000	−3.94362
	ϵ^8	154.769	1.06116	0.00000	−64.5538	0.00000	0.00000	−3.94362
	Heyliger [23]	154.765	1.06112	0.00000	−64.5526	0.00000	0.00000	−3.94337

as follows:

$$\tilde{\phi}(x_1,x_2)=\tilde{q}_{mn}\sin\tilde{m}x_1\sin\overline{n}x_2, \tag{99}$$

$$\tilde{\phi}(x_1,x_2)=\tilde{\phi}_{mn}\sin\tilde{m}x_1\sin\overline{n}x_2, \tag{100}$$

where $\overline{n}=n\pi\sqrt{h/R}/\theta_\beta$; θ_β is the angle between the two edges.

The generalized displacement components for various orders will also be expressed in the form of double Fourier series to satisfy the edge boundary conditions in advance and given by

$$u_1^k=u_{1mn}^k\cos\tilde{m}x_1\sin\overline{n}x_2, \tag{101}$$

$$u_2^k=u_{2mn}^k\sin\tilde{m}x_1\cos\overline{n}x_2, \tag{102}$$

$$u_3^k=u_{3mn}^k\sin\tilde{m}x_1\sin\overline{n}x_2, \tag{103}$$

$$D_3^k=D_{3mn}^k\sin\tilde{m}x_1\sin\overline{n}x_2. \tag{104}$$

For a cylindrical bending problem, the geometry configuration and the applied lateral loads are independent of the axial coordinate. Hence, it is reasonable to expect that the dependent field variables are also independent of axial coordinate. The relevant derivatives of the field variables with respect to the axial coordinate are identical to zeroes.

The cylindrical bending type of excitations on the lateral surfaces of the shells is further reduced as single Fourier sine series as follows:

$$\tilde{q}(x_2)=\tilde{q}_n\sin\overline{n}x_2, \tag{105}$$

Table 5
The elastic and electric field variables in a two-layer piezoelectric plate under cylindrical bending type of electric potential

ζ	ϵ^{2k}	$\overline{v}(0,\zeta)\times 10^{11}$	$\overline{w}(\frac{L}{2},\zeta)\times 10^{10}$	$\overline{\phi}(\frac{L}{2},\zeta)$	$\overline{\sigma}_y(\frac{L}{2},\zeta)$	$\overline{\tau}_{yz}(0,\zeta)$	$\overline{\sigma}_z(\frac{L}{2},\zeta)\times 10^{2}$	$\overline{D}_z(\frac{L}{2},\zeta)\times 10^{7}$
h	ϵ^0	−13.4771	4.05135	1.000000	67.6080	0.00000	0.00000	−3.50994
	ϵ^2	−17.2710	2.22403	1.000000	98.5546	0.00000	0.00000	−4.39030
	ϵ^4	−17.2280	2.21648	1.000000	98.0604	0.00000	0.00000	−4.38160
	ϵ^6	−17.2285	2.21653	1.000000	98.0665	0.00000	0.00000	−4.38171
	ϵ^8	−17.2285	2.21653	1.000000	98.0664	0.00000	0.00000	−4.38171
	Heyliger [23]	−17.2277	2.21625	1.000000	98.0706	0.00000	0.00000	−4.38016
$\frac{1}{2}h$	ϵ^0	−10.2951	4.05135	0.945228	−40.0080	1.08385	−9.78819	−3.50994
	ϵ^2	−11.6874	2.35568	0.935496	−38.9387	2.33389	−16.2316	−3.92558
	ϵ^4	−11.6680	2.37391	0.935610	−38.9891	2.30992	−16.1141	−3.91979
	ϵ^6	−11.6682	2.37364	0.935608	−38.9881	2.31024	−16.1157	−3.91987
	ϵ^8	−11.6682	2.37365	0.935608	−38.9881	2.31023	−16.1157	−3.91986
	Heyliger [23]	−11.6676	2.37336	0.935611	−38.9872	2.31044	−16.1166	−3.91847
$0^{\pm}$	ϵ^0	−7.11323	4.05135	0.887693	−147.624 (172.440)	−6.28444	5.10256	−3.50994
	ϵ^2	−6.19383	2.47484	0.874565	−176.101 (135.010)	−6.10780	−8.46081	−3.48649
	ϵ^4	−6.21199	2.49869	0.874733	−175.584 (135.730)	−6.11250	−8.20121	−3.48676
	ϵ^6	−6.21174	2.49838	0.874731	−175.591 (135.720)	−6.11243	−8.20470	−3.48676
	ϵ^8	−6.21174	2.49838	0.874731	−175.591 (135.720)	−6.11243	−8.20466	−3.48676
	Heyliger [23]	−6.21137	2.49809	0.874736	−175.593 (135.710)	−6.11227	−8.20718	−3.48550
$-\frac{1}{2}h$	ϵ^0	−3.93131	4.05135	0.444286	40.0080	2.058369	14.89075	−3.50994
	ϵ^2	−3.85727	2.72247	0.436248	38.9138	0.717910	7.76691	−3.45435
	ϵ^4	−3.85899	2.74270	0.436358	38.9441	0.744179	7.90600	−3.45512
	ϵ^6	−3.85896	2.74245	0.436357	38.9437	0.743821	7.90412	−3.45511
	ϵ^8	−3.85896	2.74246	0.436357	38.9437	0.743825	7.90414	−3.45511
	Heyliger [23]	−3.85882	2.74217	0.436359	38.9426	0.743546	7.90257	−3.45386
$-h$	ϵ^0	−0.74939	4.05135	0.000000	−92.4239	0.00000	0.00000	−3.50994
	ϵ^2	−1.53573	2.96513	0.000000	−57.3645	0.00000	0.00000	−3.44373
	ϵ^4	−1.52063	2.98164	0.000000	−58.0258	0.00000	0.00000	−3.44466
	ϵ^6	−1.52083	2.98145	0.000000	−58.0170	0.00000	0.00000	−3.44464
	ϵ^8	−1.52083	2.98145	0.000000	−58.0171	0.00000	0.00000	−3.44464
	Heyliger [23]	−1.52091	2.98116	0.00000	−58.0090	0.00000	0.00000	−3.44340

$$\tilde{\phi}(x_2)=\tilde{\phi}_n\sin\overline{n}x_2, \tag{106}$$

The generalized displacement components for various orders are also reduced to the following form

$$u_1^k=u_{1n}^k\sin\overline{n}x_2, \tag{107}$$

$$u_2^k=u_{2n}^k\cos\overline{n}x_2, \tag{108}$$

$$u_3^k=u_{3n}^k\sin\overline{n}x_2, \tag{109}$$

$$D_3^k=D_{3n}^k\sin\overline{n}x_2. \tag{110}$$

By changing the circumferential coordinate (θ) to arc length coordinate (y) with $y=R\theta$ and letting $1/R$ be zero, we may reduce the present formulation of piezoelectric cylindrical shells to that of piezoelectric plates under cylindrical bending excitations. Substituting Eqs. (107)–(110) in the governing equations of various orders and following the previous solution procedure, we finally may obtain the 3D asymptotic solutions of multilayered piezoelectric plates under electromechanical loads.

A two-layer laminate composed of [PZT-4/ceramics] with equal thickness layers is considered in Tables 4 and 5. The dimensions of length and total thickness of the plate are $L=0.1$ m and $2h=0.01$ m. The material properties of piezoelectric and ceramics layers are given in Table 1. The cylindrical bending type of either mechanical load or electric potential (i.e., $q(y)=\sin(\pi y/L)$ or $\phi(y)=\sin(\pi y/L)$) are applied on the lateral surfaces. The present asymptotic solutions of elastic and electric field components at the middle surface of each layer and at interfaces between layers are given in Tables 4 and 5 for the cases of

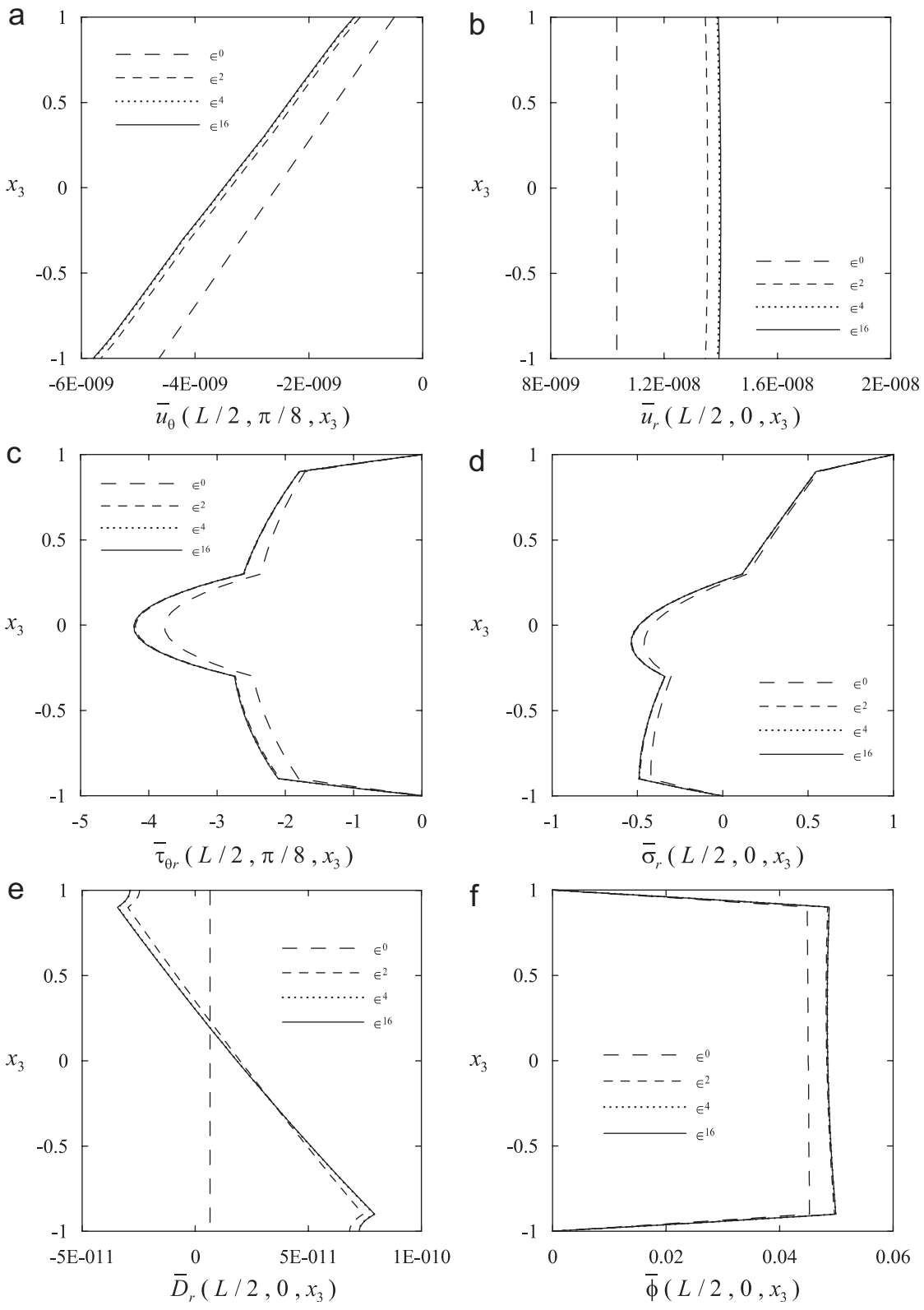

Fig. 5. The distributions of various field variables through the thickness of a multilayered piezoelectric hollow cylinder under mechanical load.

applied load and applied electric potential, respectively. The solutions are also compared with the exact solutions obtained by Heyliger and Brooks [23]. Again, it is shown that the present solutions converge rapidly and their convergent solutions are in excellent agreement with the exact solutions.

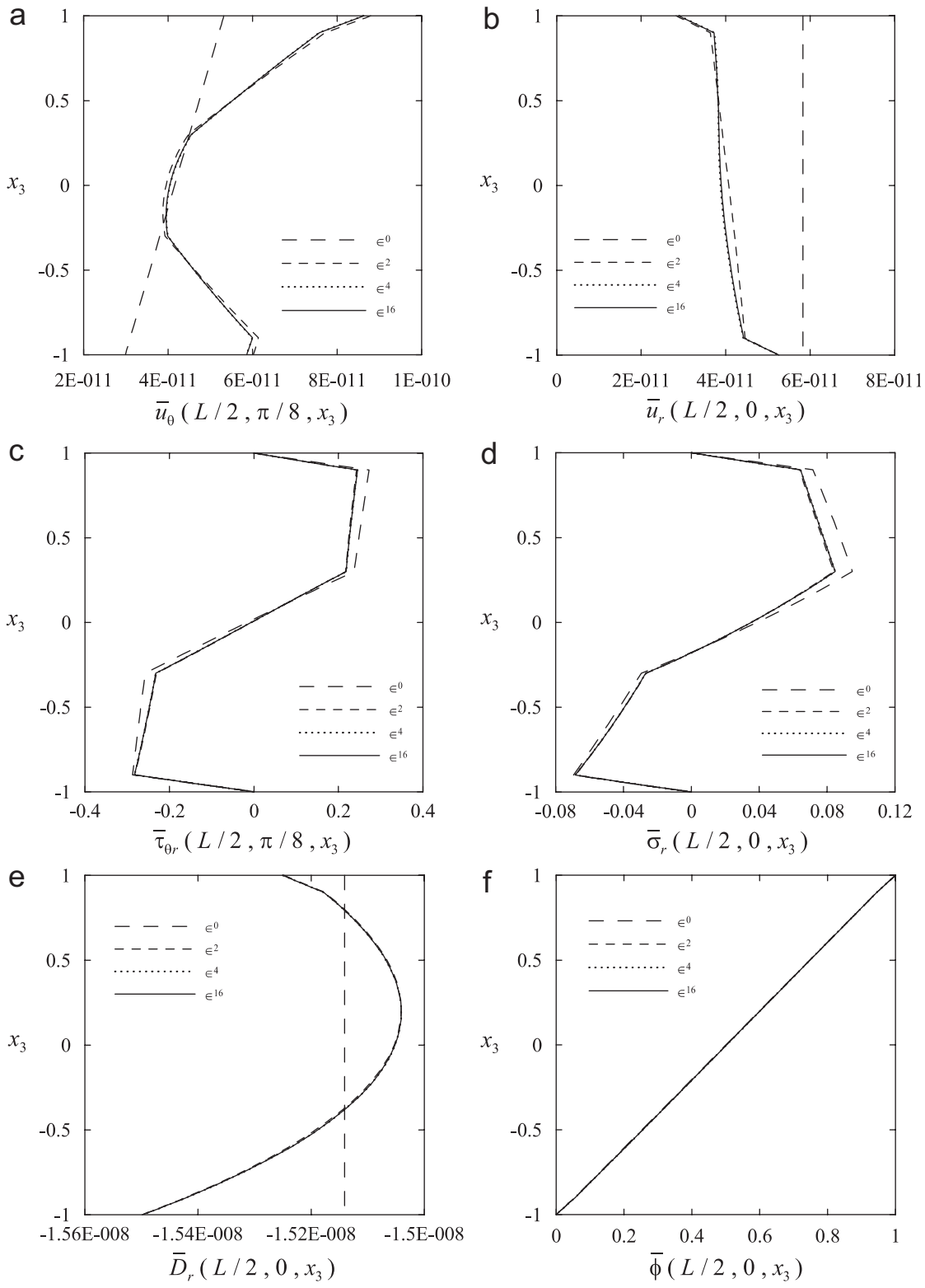

Fig. 6. The distributions of various field variables through the thickness of a multilayered piezoelectric hollow cylinder under electric potential.

6.4. Multilayered hybrid piezoelectric hollow cylinders

The piezoelectric cylinders composed of [0/90/0] laminated cylinders bonded with piezoelectric layers (PZT-4) on the outer surfaces are considered in Figs. 5 and 6 and Tables 6 and 7. Either mechanical load ($\bar{q}_r^+ = q_0 \sin(\pi x/L) \cos 4\theta$, $q_0 = -1\,\mathrm{N/m^2}$) or electric potential ($\bar{\Phi}^+ = \phi_0 \sin(\pi x/L) \cos 4\theta$, $\phi_0 = 1\,\mathrm{V}$) is applied on the lateral surfaces.

Table 6
The elastic and electric field variables at crucial positions of multilayered hybrid piezoelectric hollow cylinders under lateral load

$R/2h$	x_3	$\overline{u}_\theta(\frac{L}{2},\frac{\pi}{8},x_3)$	$\overline{u}_r(\frac{L}{2},0,x_3)$	$\overline{\sigma}_\theta(\frac{L}{2},0,x_3)$	$\overline{\tau}_{x\theta}(0,\frac{\pi}{8},x_3)$	$\overline{\tau}_{\theta r}(\frac{L}{2},\frac{\pi}{L},x_3)$	$\overline{\sigma}_r(\frac{L}{2},0,x_3)$	$\overline{\phi}(\frac{L}{2},0,x_3)$	$\overline{D}_r(\frac{L}{2},0,x_3)$
5	h	−1.3750e−11	1.2579e−09	24.8090	2.3349	0.0000	1.0000	0.0000	−1.7236e−11
	$0.95h$	−3.6390e−11	1.2606e−09	23.0970	2.1273	−0.4473	8.9089e−01	6.0155e−03	−1.8629e−11
	$0.9h^{\pm}$	−5.8709e−11	1.2631e−09	21.3880	1.9218	−0.8685	7.8033e−01	1.1617e−02	−2.2575e−11
				(2.2587)	(0.4503)				
	$0.6h$	−1.4393e−10	1.2627e−09	1.5854	0.2343	−1.1469	6.2798e−01	1.1468e−02	−7.6879e−12
	$0.3h^{\pm}$	−2.1768e−10	1.2615e−09	0.9606	0.0357	−1.3682	4.5430e−01	1.1471e−02	8.3808e−12
				(13.9880)	(0.0357)				
	0	−3.1800e−10	1.2611e−09	−0.3704	−0.1268	−2.2654	2.5134e−02	1.1638e−02	2.5996e−11
	$-0.3h^{\pm}$	−4.1824e−10	1.2594e−09	−15.4880	−0.2930	−1.4483	3.7437e−03	1.1987e−02	4.5616e−11
				(−0.8673)	(−0.2930)				
	$-0.6h$	−4.8777e−10	1.2547e−09	−1.5788	−0.5018	−1.3752	−1.4699e−01	1.2540e−02	6.7816e−11
	$-0.9h^{\pm}$	−5.6555e−10	1.2480e−09	−2.4018	−0.7356	−1.1875	−2.6393e−01	1.3327e−02	9.3333e−11
				(−24.1360)	(−3.1392)				
	$-0.95h$	−5.8907e−10	1.2451e−09	−26.5580	−3.3826	−0.6262	−1.4626e−01	7.0109e−03	8.7455e−11
	$-h$	−6.1302e−10	1.2419e−09	−29.0390	−3.6322	0.0000	0.0000	0.0000	8.5701e−11
10	h	−1.2039e−09	1.3916e−08	97.2340	8.1958	0.0000	1.0000	0.0000	−2.8875e−11
	$0.95h$	−1.3332e−09	1.3927e−08	92.0410	7.5928	−0.9201	0.7719	2.5017e−02	−3.0298e−11
	$0.9h^{\pm}$	−1.4619e−09	1.3938e−08	86.8450	6.9914	−1.7958	0.5463	4.8750e−02	−3.4355e−11
				(8.3971)	(1.6382)				
	$0.6h$	−2.1357e−09	1.3968e−08	5.7282	0.8633	−2.2780	0.3266	4.8495e−02	−1.7459e−11
	$0.3h^{\pm}$	−2.7914e−09	1.3989e−08	3.0503	0.0981	−2.6133	0.1135	4.8409e−02	1.1227e−13
				(50.7480)	(0.0981)				
	0	−3.5014e−09	1.4002e−08	−0.1475	−0.6388	−4.2179	−0.4918	4.8500e−02	1.8460e−11
	$-0.3h^{\pm}$	−4.2113e−09	1.4002e−08	−52.5330	−1.3898	−2.7427	−0.3401	4.8774e−02	3.7698e−11
				(−3.0240)	(−1.3898)				
	$-0.6h$	−4.8621e−09	1.3987e−08	−5.9336	−2.1881	−2.5286	−0.4481	4.9242e−02	5.7953e−11
	$-0.9h^{\pm}$	−5.5302e−09	1.3958e−08	−9.0008	−3.0163	−2.1060	−0.4912	4.9914e−02	7.9370e−11
				(−92.0470)	(−12.8730)				
	$-0.95h$	−5.6604e−09	1.3947e−08	−98.2890	−13.5330	−1.0907	−0.2602	2.5825e−02	7.4231e−11
	$-h$	−5.7915e−09	1.3935e−08	−104.5900	−14.1990	0.0000	0.0000	0.0000	7.2586e−11

The thickness ratio of each layer is PZT-4 : 0°-layer:90°-layer:0°-layer:PZT-4 = 0.1 h: 0.6h:0.6h:0.6h:0.1h. The elastic, piezoelectric and dielectric properties of composite (Graphite/Epoxy) and piezoelectric (PZT-4) materials [22] are given in Table 1. The geometry parameters are taken as $L/R = 4$; $R/2h = 5$, 10 in Tables 4 and 5 and $R/2h = 10$ in Figs. 5 and 6. The sets of dimensionless variables in the cases of applied mechanical loads and applied potentials used in Example 6.2 are adopted. Figs. 5 and 6 show the through-thickness distributions of the present asymptotic solutions of elastic and electric field variables for various orders. It is shown that the present asymptotic solutions converge rapidly. In addition, the asymptotic solutions yield continuous interlaminar out-of-surface field variables. The lateral boundary conditions are satisfied exactly. The maximum values of transverse stresses occur in the vicinity of middle surface of the 90°-layer in the case of applied load and at the interfaces between two dissimilar layers in the case of applied potential. In the cases of applied potential, the distributions of displacements through the thickness coordinate reveal approximately a layerwise linear or higher-degree polynomial function and not coincide with the basic kinematics assumptions of CST. CST may be not appropriate for the analysis of multilayered piezoelectric shells especially when they are under electric loads. The present convergent solutions of elastic and electric field variables at the middle surface of each layer and at interfaces of layers are tabulated in Tables 6 and 7 for the cases of applied load and applied electric potential, respectively. The present solutions in Table 6 and 7 can be provided as the benchmark solutions for assessing various approximate 2D shell theories.

7. Conclusions

By means of an asymptotic approach, we present 3D solutions of mechanical and electrical field variables for multilayered piezoelectric hollow cylinders under either the lateral loads or the lateral potentials. The present solutions of both piezoelectric cylinders under axisymmetric excitations and multilayered piezoelectric plates under cylindrical bending excitations are illustrated to converge rapidly and their convergent solutions are in excellent agreement with the exact solutions available in the literature. A parametric study on the static analysis of multilayered piezoelectric cylinders is presented. It is noted that the distributions of field variables through the thickness of the shell dramatically change in the cases of applied potentials,

Table 7
The elastic and electric field variables at crucial positions of multilayered hybrid piezoelectric hollow cylinders under lateral potential

$R/2h$	x_3	$\bar{u}_\theta(\frac{L}{2},\frac{\pi}{8},x_3)$	$\bar{u}_r(\frac{L}{2},0,x_3)$	$\bar{\sigma}_\theta(\frac{L}{2},0,x_3)$	$\bar{\tau}_{x\theta}(0,\frac{\pi}{8},x_3)$	$\bar{\tau}_{\theta r}(\frac{L}{2},\frac{\pi}{L},x_3)$	$\bar{\sigma}_r(\frac{L}{2},0,x_3)$	$\bar{\phi}(\frac{L}{2},0,x_3)$	$\bar{D}_r(\frac{L}{2},0,x_3)$
5	h	8.7323e−11	1.7236e−11	−11.2040	0.9998	0.0000	0.0000	1.0000	−1.6837e−08
	$0.95h$	7.7566e−11	2.2148e−11	−11.6200	0.9104	0.2051	5.4043e−02	0.9708	−1.6647e−08
	$0.9h^{\pm}$	6.7781e−11	2.6925e−11	−12.0470	0.8204	0.4212	1.1455e−01	0.9418	−1.6460e−08
				(0.6143)	(0.1922)				
	$0.6h$	4.2312e−11	2.7723e−11	0.4439	0.1557	0.3805	1.4967e−01	0.7840	−1.5765e−08
	$0.3h^{\pm}$	1.9082e−11	2.7173e−11	0.2792	0.1251	0.3568	1.8709e−01	0.6322	−1.5219e−08
				(3.7324)	(0.1251)				
	0	1.1992e−11	2.6283e−11	2.7521	0.1137	−0.0086	1.1842e−01	0.4850	−1.4835e−08
	$-0.3h^{\pm}$	1.2142e−11	2.6319e−11	2.8213	0.1153	−0.3508	1.6682e−02	0.3407	−1.4637e−08
				(0.1732)	(0.1153)				
	$-0.6h$	2.7843e−11	2.7720e−11	0.3008	0.1360	−0.4070	−3.9106e−02	0.1974	−1.4649e−08
	$-0.9h^{\pm}$	4.6147e−11	3.0749e−11	0.4597	0.1638	−0.4884	−1.1301e−01	0.0527	−1.4906e−08
				(−11.2700)	(0.6992)				
	$-0.95h$	4.5097e−11	3.5028e−11	−11.2930	0.6928	−0.2465	−5.9669e−02	0.0264	−1.4977e−08
	$-h$	4.4001e−11	3.9317e−11	−11.3260	0.6860	0.0000	0.0000	0.0000	−1.5057e−08
10	h	8.6273e−11	2.8875e−11	−12.8110	0.7567	0.0000	0.0000	1.0000	−1.5250e−08
	$0.95h$	8.1045e−11	3.3059e−11	−12.9220	0.7334	0.1215	3.1308e−02	0.9728	−1.5214e−08
	$0.9h^{\pm}$	7.5788e−11	3.7210e−11	−13.0360	0.7099	0.2450	6.4249e−02	0.9457	−1.5178e−08
				(0.3688)	(0.1663)				
	$0.6h$	6.0221e−11	3.8016e−11	0.3151	0.1561	0.2302	7.4455e−02	0.7974	−1.5088e−08
	$0.3h^{\pm}$	4.5499e−11	3.8413e−11	0.2629	0.1473	0.2181	8.4735e−02	0.6497	−1.5044e−08
				(3.9896)	(0.1473)				
	0	4.0371e−11	3.8961e−11	3.6672	0.1442	−0.0069	3.5344e−02	0.5022	−1.5052e−08
	$-0.3h^{\pm}$	3.9868e−11	4.0180e−11	3.6847	0.1453	−0.2326	−2.6956e−02	0.3544	−1.5114e−08
				(0.2102)	(0.1453)				
	$-0.6h$	4.9418e−11	4.1964e−11	0.2496	0.1523	−0.2560	−4.6239e−02	0.2057	−1.5235e−08
	$-0.9h^{\pm}$	5.9951e−11	4.4254e−11	0.2943	0.1609	−0.2831	−6.8576e−02	0.0554	−1.5421e−08
				(−13.6830)	(0.6868)				
	$-0.95h$	5.9300e−11	4.8436e−11	−13.6820	0.6854	−0.1421	−3.5144e−02	0.0278	−1.5459e−08
	$-h$	5.8611e−11	5.2623e−11	−13.6850	0.6839	0.0000	0.0000	0.0000	-1.5499e−08

especially in thick shells. The advanced shell theory used for the piezoelectric analysis is more necessary than that used for the elastic analysis.

Acknowledgment

This work is supported by the National Science Council of Republic of China through Grant NSC 94-2211-E006-051.

Appendix A

The relevant functions $\tilde{l}_{ij}$ in Eqs. (14)–(19) are given as follows:

$$\tilde{l}_{31}=\left(\frac{e_{31}e_{33}+c_{13}\eta_{33}}{e_{33}^2+c_{33}\eta_{33}}\right)\frac{\partial}{\partial x_1}+\left(\frac{e_{36}e_{33}+c_{36}\eta_{33}}{e_{33}^2+c_{33}\eta_{33}}\right)\frac{1}{\gamma_\theta}\frac{\partial}{\partial x_2}, \tag{A.1}$$

$$\tilde{l}_{32}=\left(\frac{e_{36}e_{33}+c_{36}\eta_{33}}{e_{33}^2+c_{33}\eta_{33}}\right)\frac{\partial}{\partial x_1}+\left(\frac{e_{32}e_{33}+c_{23}\eta_{33}}{e_{33}^2+c_{33}\eta_{33}}\right)\frac{1}{\gamma_\theta}\frac{\partial}{\partial x_2}, \tag{A.2}$$

$$\tilde{l}_{33}=\left(\frac{e_{32}e_{33}+c_{23}\eta_{33}}{e_{33}^2+c_{33}\eta_{33}}\right)\frac{1}{\gamma_\theta}, \tag{A.3}$$

$$\tilde{l}_{34}=\frac{\eta_{33}Q}{e_{33}^2+c_{33}\eta_{33}}, \tag{A.4}$$

$$\tilde{l}_{35}=\frac{e_{33}e}{e_{33}^2+c_{33}\eta_{33}}, \tag{A.5}$$

$$\tilde{l}_{22}=(1-x_3\partial_3), \tag{A.6}$$

$$\tilde{l}_{26}=-x_3Qc_{45}/(c_{44}c_{55}-c_{45}^2), \tag{A.7}$$

$$\tilde{l}_{27}=x_3Qc_{55}/(c_{44}c_{55}-c_{45}^2), \tag{A.8}$$

$$\tilde{l}_{14}=\frac{c_{44}Q}{c_{44}c_{55}-c_{45}^2}, \tag{A.9}$$

$$\tilde{l}_{15}=-\frac{c_{45}Q}{c_{44}c_{55}-c_{45}^2}, \tag{A.10}$$

$$\tilde{l}_{25}=\frac{c_{55}Q}{c_{44}c_{55}-c_{45}^2}, \tag{A.11}$$

$$\tilde{l}_{18}=\left(\frac{c_{45}e_{14}-c_{44}e_{15}}{c_{44}c_{55}-c_{45}^2}\right)\frac{Q}{e}\frac{\partial}{\partial x_1}+\left(\frac{c_{45}e_{24}-c_{44}e_{25}}{c_{44}c_{55}-c_{45}^2}\right)\frac{Q}{e\gamma_\theta}\frac{\partial}{\partial x_2}, \tag{A.12}$$

$$\tilde{l}_{28}=\left(\frac{c_{45}e_{15}-c_{55}e_{14}}{c_{44}c_{55}-c_{45}^2}\right)\frac{Q\gamma_\theta}{e}\frac{\partial}{\partial x_1}+\left(\frac{c_{45}e_{25}-c_{55}e_{24}}{c_{44}c_{55}-c_{45}^2}\right)\frac{Q}{e}\frac{\partial}{\partial x_2}, \tag{A.13}$$

$$\tilde{l}_{41}=\tilde{Q}_{11}\gamma_\theta\frac{\partial^2}{\partial x^2}+(\tilde{Q}_{16}+\tilde{Q}_{61})\frac{\partial^2}{\partial x_1\partial x_2}+\frac{\tilde{Q}_{66}}{\gamma_\theta}\frac{\partial^2}{\partial x_2^2}, \tag{A.14}$$

$$\tilde{l}_{42}=\tilde{Q}_{16}\gamma_\theta\frac{\partial^2}{\partial x_1^2}+(\tilde{Q}_{12}+\tilde{Q}_{66})\frac{\partial^2}{\partial x_1\partial x_2}+\frac{\tilde{Q}_{62}}{\gamma_\theta}\frac{\partial^2}{\partial x_2^2}, \tag{A.15}$$

$$\tilde{l}_{51}=\tilde{Q}_{61}\gamma_\theta\frac{\partial^2}{\partial x_1^2}+(\tilde{Q}_{21}+\tilde{Q}_{66})\frac{\partial^2}{\partial x_1\partial x_2}+\frac{\tilde{Q}_{26}}{\gamma_\theta}\frac{\partial^2}{\partial x_2^2}, \tag{A.16}$$

$$\tilde{l}_{52}=\tilde{Q}_{66}\gamma_\theta\frac{\partial^2}{\partial x_1^2}+(\tilde{Q}_{26}+\tilde{Q}_{62})\frac{\partial^2}{\partial x_1\partial x_2}+\frac{\tilde{Q}_{22}}{\gamma_\theta}\frac{\partial^2}{\partial x_2^2}, \tag{A.17}$$

$$\tilde{l}_{43}=\tilde{Q}_{12}\frac{\partial}{\partial x_1}+\frac{\tilde{Q}_{62}}{\gamma_\theta}\frac{\partial}{\partial x_2}, \tag{A.18}$$

$$\tilde{l}_{53}=\tilde{Q}_{62}\frac{\partial}{\partial x_1}+\frac{\tilde{Q}_{22}}{\gamma_\theta}\frac{\partial}{\partial x_2}, \tag{A.19}$$

$$\tilde{l}_{44}=1+x_3\frac{\partial}{\partial x_3}, \tag{A.20}$$

$$\tilde{l}_{55}=2+x_3\frac{\partial}{\partial x_3}, \tag{A.21}$$

$$\tilde{l}_{46}=\left(\frac{c_{13}e_{33}-e_{31}c_{33}}{e_{33}^2+c_{33}\eta_{33}}\right)\frac{\gamma_\theta e}{Q}\frac{\partial}{\partial x_1}+\left(\frac{c_{36}e_{33}-e_{36}c_{33}}{e_{33}^2+c_{33}\eta_{33}}\right)\frac{e}{Q}\frac{\partial}{\partial x_2}, \tag{A.22}$$

$$\tilde{l}_{56}=\left(\frac{c_{36}e_{33}-e_{36}c_{33}}{e_{33}^2+c_{33}\eta_{33}}\right)\frac{\gamma_\theta e}{Q}\frac{\partial}{\partial x_1}+\left(\frac{c_{23}e_{33}-e_{32}c_{33}}{e_{33}^2+c_{33}\eta_{33}}\right)\frac{e}{Q}\frac{\partial}{\partial x_2}, \tag{A.23}$$

$$\tilde{l}_{61}=\tilde{Q}_{21}\frac{\partial}{\partial x_1}+\frac{\tilde{Q}_{26}}{\gamma_\theta}\frac{\partial}{\partial x_2}, \tag{A.24}$$

$$\tilde{l}_{62}=\tilde{Q}_{26}\frac{\partial}{\partial x_1}+\frac{\tilde{Q}_{22}}{\gamma_\theta}\frac{\partial}{\partial x_2}, \tag{A.25}$$

$$\tilde{l}_{63}=\frac{\tilde{Q}_{22}}{\gamma_\theta}, \tag{A.26}$$

$$\tilde{l}_{64}=1+x_3\frac{\partial}{\partial x_3}-\left(\frac{e_{32}e_{33}+c_{23}\eta_{33}}{e_{33}^2+c_{33}\eta_{33}}\right), \tag{A.27}$$

$$\tilde{l}_{65}=\frac{e}{Q}\left(\frac{c_{23}e_{33}-e_{32}c_{33}}{e_{33}^2+c_{33}\eta_{33}}\right), \tag{A.28}$$

$$\tilde{l}_{71}=\frac{1}{\gamma_\theta}, \tag{A.29}$$

$$\tilde{l}_{81}=\left(\frac{c_{33}}{e_{33}^2+c_{33}\eta_{33}}\right)\frac{e^2}{Q}, \tag{A.30}$$

$$\tilde{Q}_{ij}=\frac{Q_{ij}}{Q}\quad\text{and}\quad Q_{ij}=c_{ij}-\left(\frac{e_{33}e_{3j}+c_{j3}\eta_{33}}{e_{33}^2+c_{33}\eta_{33}}\right)\times c_{i3}-\left(\frac{e_{33}c_{j3}-c_{33}e_{3j}}{e_{33}^2+c_{33}\eta_{33}}\right)e_{3i}\,(i,j=1,2,6). \tag{A.31}$$

The relevant functions $\tilde{b}_{ij}$ in Eqs. (20)–(21) are given by

$$\tilde{b}_{11}=\tilde{Q}_{11}\frac{\partial}{\partial x_1}+\frac{\tilde{Q}_{16}}{\gamma_\theta}\frac{\partial}{\partial x_2},\quad \tilde{b}_{12}=\tilde{Q}_{16}\frac{\partial}{\partial x_1}+\frac{\tilde{Q}_{12}}{\gamma_\theta}\frac{\partial}{\partial x_2}, \tag{A.32–A.33}$$

$$\tilde{b}_{21}=\tilde{Q}_{21}\frac{\partial}{\partial x_1}+\frac{\tilde{Q}_{26}}{\gamma_\theta}\frac{\partial}{\partial x_2},\quad \tilde{b}_{22}=\tilde{Q}_{26}\frac{\partial}{\partial x_1}+\frac{\tilde{Q}_{22}}{\gamma_\theta}\frac{\partial}{\partial x_2}, \tag{A.34–A.35}$$

$$\tilde{b}_{31}=\tilde{Q}_{61}\frac{\partial}{\partial x_1}+\frac{\tilde{Q}_{66}}{\gamma_\theta}\frac{\partial}{\partial x_2},\quad \tilde{b}_{32}=\tilde{Q}_{66}\frac{\partial}{\partial x_1}+\frac{\tilde{Q}_{62}}{\gamma_\theta}\frac{\partial}{\partial x_2}, \tag{A.36–A.37}$$

$$\tilde{b}_{13}=\frac{\tilde{Q}_{12}}{\gamma_\theta},\quad \tilde{b}_{23}=\frac{\tilde{Q}_{22}}{\gamma_\theta},\quad \tilde{b}_{33}=\frac{\tilde{Q}_{62}}{\gamma_\theta}, \tag{A.38–A.40}$$

$$\tilde{b}_{14}=\frac{e_{31}e_{33}+c_{13}\eta_{33}}{e_{33}^2+c_{33}\eta_{33}},\quad \tilde{b}_{24}=\frac{e_{32}e_{33}+c_{23}\eta_{33}}{e_{33}^2+c_{33}\eta_{33}}, \tag{A.41–A.42}$$

$$\tilde{b}_{34}=\frac{e_{36}e_{33}+c_{36}\eta_{33}}{e_{33}^2+c_{33}\eta_{33}}, \tag{A.43}$$

$$\tilde{b}_{15}=(e/Q)\frac{c_{13}e_{33}-e_{31}c_{33}}{e_{33}^2+c_{33}\eta_{33}},\quad \tilde{b}_{25}=(e/Q)\frac{c_{23}e_{33}-e_{32}c_{33}}{e_{33}^2+c_{33}\eta_{33}}, \tag{A.44–A.45}$$

$$\tilde{b}_{35}=(e/Q)\frac{c_{36}e_{33}-e_{36}c_{33}}{e_{33}^2+c_{33}\eta_{33}}, \tag{A.46}$$

$$\tilde{b}_{41} = (Q/e)\frac{c_{44}e_{15} - c_{45}e_{14}}{c_{44}c_{55} - c_{45}^2},$$

$$\tilde{b}_{42} = (Q/e)\frac{c_{55}e_{14} - c_{45}e_{15}}{c_{44}c_{55} - c_{45}^2}, \quad \text{(A.47–A.48)}$$

$$\tilde{b}_{51} = (Q/e)\frac{c_{44}e_{25} - c_{45}e_{24}}{c_{44}c_{55} - c_{45}^2},$$

$$\tilde{b}_{52} = (Q/e)\frac{c_{55}e_{24} - c_{45}e_{25}}{c_{44}c_{55} - c_{45}^2}, \quad \text{(A.49–A.50)}$$

$$\tilde{b}_{43} = \left[\left(\frac{c_{45}e_{15} - c_{55}e_{14}}{c_{44}c_{55} - c_{45}^2}\right)e_{14} + \left(\frac{c_{45}e_{14} - c_{44}e_{15}}{c_{44}c_{55} - c_{45}^2}\right)e_{15} - \eta_{11}\right]\frac{Q}{e^2}\frac{\partial}{\partial x_1} + \left[\left(\frac{c_{45}e_{25} - c_{55}e_{24}}{c_{44}c_{55} - c_{45}^2}\right)e_{14} + \left(\frac{c_{45}e_{24} - c_{44}e_{25}}{c_{44}c_{55} - c_{45}^2}\right)e_{15} - \eta_{12}\right]\frac{Q}{e^2\gamma_\theta}\frac{\partial}{\partial x_2}, \quad \text{(A.51)}$$

$$\tilde{b}_{53} = \left[\left(\frac{c_{45}e_{15} - c_{55}e_{14}}{c_{44}c_{55} - c_{45}^2}\right)e_{24} + \left(\frac{c_{45}e_{14} - c_{44}e_{15}}{c_{44}c_{55} - c_{45}^2}\right)e_{25} - \eta_{12}\right]\frac{Q}{e^2}\frac{\partial}{\partial x_1} + \left[\left(\frac{c_{45}e_{25} - c_{55}e_{24}}{c_{44}c_{55} - c_{45}^2}\right)e_{24} + \left(\frac{c_{45}e_{24} - c_{44}e_{25}}{c_{44}c_{55} - c_{45}^2}\right)e_{25} - \eta_{22}\right]\frac{Q}{e^2\gamma_\theta}\frac{\partial}{\partial x_2}. \quad \text{(A.52)}$$

References

[1] Heyliger P. Static behavior of laminated elastic/piezoelectric plates. AIAA Journal 1994;32(12):2481–4.

[2] Heyliger P. Exact solutions for simply supported laminated piezoelectric plates. Journal of Applied Mechanics 1997;64(2):299–306.

[3] Xu K, Noor AK, Tang YY. Three-dimensional solutions for coupled thermoelectroelastic response of multilayered plates. Computer Methods in Applied Mechanics and Engineering 1995;126:355–71.

[4] Dumir PC, Dube GP, Kapuria S. Exact piezoelastic solution of simply-supported orthotropic circular cylindrical panel in cylindrical bending. International Journal of Solids and Structures 1997;34(6):685–702.

[5] Dube GP, Kapuria S, Dumir PC. Exact piezothermoelastic solution of simply-supported orthotropic circular cylindrical panel in cylindrical bending. Archive of Applied Mechanics 1996;66:537–54.

[6] Chen CQ, Shen YP, Wang XM. Exact solution of orthotropic cylindrical shell with piezoelectric layers under cylindrical bending. International Journal of Solids and Structures 1996;33(30):4481–94.

[7] Chen C, Shen Y, Liang X. Three dimensional analysis of piezoelectric circular cylindrical shell of finite length. Acta Mechanica 1999;134(3):235–49.

[8] Heyliger P. A note on the static behavior of simply-supported laminated piezoelectric cylinders. International Journal of Solids Structures 1997;34(29):3781–94.

[9] Kapuria S, Sengupta S, Dumir PC. Three-dimensional solution for a hybrid cylindrical shell under axisymmetric thermoelectric load. Archive of Applied Mechanics 1997;67:320–30.

[10] Kapuria S, Dumir PC, Sengupta S. Nonaxisymmetric exact piezothermoelastic solution for laminated cylindrical shell. AIAA Journal 1997;35(11):1792–5.

[11] Xu KM, Noor AK. Three-dimensional analytical solutions for coupled thermoelectroelastic response of multilayered cylindrical shells. AIAA Journal 1996;34:802–10.

[12] Kapuria S, Sengupta S, Dumir PC. Assessment of shell theories for hybrid piezoelectric cylindrical shell under electromechanical load. International Journal of Mechanical Sciences 1998;40(5):461–77.

[13] Gopinathan SV, Varadan VV, Varadan VK. A review and critique of theories for piezoelectric laminates. Smart Materials and Structures 2000;9(1):24–48.

[14] Chee CYK, Tong L, Steven GP. A review on modeling of piezoelectric sensors and actuators incorporated in intelligent structures. Journal of Intelligent Material Systems and Structures 1998;9(1):3–19.

[15] Wu CP, Tarn JQ, Chi SM. An asymptotic theory for dynamic response of doubly curved laminated shells. International Journal of Solids and Structures 1996;33(26):3813–41.

[16] Wu CP, Chiu SJ. Thermally induced dynamic instability of laminated composite conical shells. International Journal of Solids and Structures 2002;39(11):3001–21.

[17] Wu CP, Chi YW. Three-dimensional nonlinear analysis of laminated cylindrical shells under cylindrical bending. European Journal of Mechanics A/Solids 2005;24(5):837–56.

[18] Heyliger P, Saravanos DA. Exact free-vibration analysis of laminated plates with embedded piezoelectric layers. Journal of the Acoustical Society of America 1995;98(3):1547–57.

[19] Vel SS, Batra RC. Exact solution for the cylindrical bending of laminated plates with embedded piezoelectric shear actuators. Smart Materials and Structures 2001;10:240–51.

[20] Sun CT, Zhang XD. Use of thickness-shear mode in adaptive sandwich structures. Smart Materials and Structures 1995;4:202–6.

[21] Kapuria S, Sengupta S, Dumir PC. Three-dimensional solution for simply-supported piezoelectric cylindrical shell for axisymmetric load. Computer Methods in Applied Mechanics and Engineering 1997;140:139–55.

[22] Vel SS, Mewer RC, Batra RC. Analytical solution for the cylindrical bending vibration of piezoelectric composite plates. International Journal of Solids and Structures 2004;41:1625–43.

[23] Heyliger P, Brooks S. Exact solutions for laminated piezoelectric plates in cylindrical bending. Journal of Applied Mechanics 1996;63:903–10.